ELECTRONIC SUPPLEMENTARY INFORMATION

Contorted Tetrabenzoacenes of Varied Conjugation: Charge Transport Study with Single-Crystal Field-Effect Transistors

Ding-Chi Huang,[†] Chi-Hsien Kuo,[‡] Man-Tzu Ho,[§] Bo-Chao Lin,[‡] Wei-Tao Peng,[‖] Ito Chao,[‡] Chao-Ping Hsu,*[,‡] Yu-Tai Tao*[,†,‡]

[†] Department of Chemistry, National Tsing-Hua University, Hsin-chu, Taiwan
[‡] Institute of Chemistry, Academia Sinica, Taipei, Taiwan
[§] Department of Chemistry, National Central University, Chung-Li, Taiwan
[‖] Department of Chemistry, Michigan State University, East Lansing, MI, USA 48824

Email: ytt@gate.sinica.edu.tw

Table of Contents:

(A)	Synthetic procedure and analytic data	S2
(B)	NMR spectra	S6
(C)	Computational details	S14
(D)	Optic microscope images of Crystals	S34
(E)	Device picture, output characteristics and transfer characteristics of SCFET devices	S34
(F)	Reference	S36

(A) **Synthetic procedures and characterization**

All chemicals were purchased from Acros, Alfa Aesar, Matrix, Merck, and Sigma-Aldrich respectively. All reactions were carried out using conventional Schlenkware technique under nitrogen atmosphere. ^{1}H and ^{13}C NMR spectra were recorded with Bruker AV400, AV500 or AVⅢ-500 spectrometer. The proton and carbon chemical shifts (δ) are reported in ppm relative to the residual signals for $CDCl_3$ (^{1}H- 7.24; ^{13}C-77.00), CD_2Cl_2 (5.32), or d_6-DMSO (2.50) ppm at room temperature, or CD_2Cl_4 (^{1}H-6.00) at high temperature NMR (343K). Mass spectra were recorded by HR-FAB/HR-EI method on a JMS-700 double focusing mass spectrometer (JEOL, Tokyo, Japan). MALDI mass spectrometry was recorded with Applied Biosystems 4800 Proteomics Analyzer (Applied Biosystem, Foster City) and HR ESI (Electrospray) spectra was recorded with dual ionization ESCi® (ESI/APCi) source options, Waters LCT Premier XE (Waters Corp., Manchester, UK).

Compound **TBN**

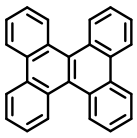

The same synthetic procedures from fluorenone derivatives to tetrabenzoacenes were used for **TBN** series of compounds. That for **TBN** are described in detail as an example. A solution containing 9-fluorenone (3 g, 16.6 mmol), zinc powder (17.4 g, 266 mmol) and zinc chloride (3.2 g, 23.3 mmol) in THF/ H_2O (30 / 3 mL) was stirred at 25 °C for 1 h. Then the solution was extracted with ethyl acetate. The organic layer was dried over anhydrous $MgSO_4$. After separation of the drying agent, the solvent was evaporated, dried benzene (300 mL) and trifluoromethanesulfonic acid (30 mL) were added to the residue. The mixture was stirred at refluxing temperature under nitrogen for two days. The reaction was quenched by water, after which benzene was removed by rotary evaporator. The residue was washed by water and directly purified by vacuum sublimation (10^{-5} torr) to give the pure product as white solid (1.8 g, yield = 70%). ^{1}H NMR (500M Hz, $CDCl_3$, δ):8.70- 8.68 (m, 8H), 7.68- 7.60 (m, 8H); ^{13}C NMR (125M Hz, $CDCl_3$, δ): 130.87, 129.23, 128.89, 127.49, 126.53 (2), 123.58; HRMS (FAB) (m/z): $[M]^+$ cal. for $C_{26}H_{16}$: 328.1252, found: 328.1245.

Compound **TBT**

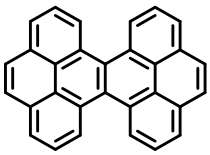

The procedures for preparing **TBT** were the same as that for **TBN**.
Orange solid, yield = 55%, ^{1}H NMR (500M Hz, $CDCl_3$, δ): 9.23 (d, *J* = 8.0 Hz, 4H); 8.24 (d, *J* = 7.5 Hz, 4H), 8.13 (s, 4H), 8.06 (dd, *J* = 7.5, 8.0 Hz, 4H); ^{13}C NMR (125M Hz, $CDCl_3$, δ): 131.35, 128.96, 128.61, 127.40, 126.00, 125.64, 125.45, 124.91; HRMS (FAB) (m/z): $[M]^+$ cal. for $C_{30}H_{16}$: 376.1252, found: 376.1252.

Compound **TBH**

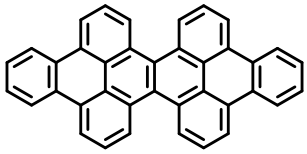

The procedures for preparing **TBH** were the same as that for **TBN**.
Orange solid, yield = 62%, ^{1}H NMR (500M Hz, $CDCl_3$, δ): 9.12 (d, *J* = 7.5 Hz, 4H), 8.95 (d, *J* = 7.5 Hz, 4H), 8.90 -8.89 (m, 4H), 8.05 (t, *J* = 7.5 Hz, 4H), 7.79 -7.77 (m, 4H); ^{13}C NMR (125M Hz, $CDCl_3$, δ): 130.18, 129.29, 129.19, 128.14, 127.64, 127.11, 125.83, 124.54, 123.75, 120.51; HRMS (MALDI) (m/z): $[M]^+$ cal. for $C_{38}H_{20}$:476.1565 , found: 476.1577.

Compound **TBO**

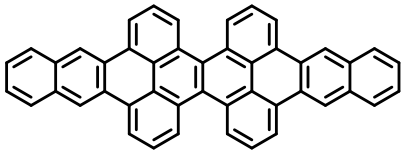

The procedures for preparing **TBO** were the same as that for **TBN**.
Orange solid, yield = 45%, ^{1}H NMR (500M Hz, $C_2D_2Cl_4$, 343K, δ): 9.39(s, 4H); 9.19-9.15 (m, 8H); 8.26- 8.24 (m, 4H); 8.15 (t, *J*= 7.8 Hz, 4H,), 7.70- 7.68 (m, 4H); Compound **TBO** was sparingly soluble to give a ^{13}C-NMR spectrum; HRMS (MALDI) (m/z): [M+H]+ cal. for $C_{46}H_{24}$: 576.1878, found: 576.1892.

Compound **3**

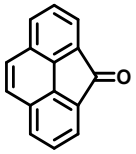

The 4, 5-phenanthrene dicarboxylic acid (5 g, 18.7 mmol) were treated with 2 N aqueous sodium hydroxide solution (20 mL) to form clear brown solution. Barium hydroxide octahydrate (6 g, 19mmol) was added and the light brown precipitates were filtered by suction and washed by water. The filtered cake was dried under vacuum,

then heated at 400°C under vacuum (0.3 torr) for 1 h. Yellow crystals formed during the pyrolysis. The solid was collected and purified by column chromatography on silica gel column using hexane: dichloromethane (1:1) as the eluent to give the target product as yellow solid (1.34 g, 35%). ^{1}H NMR (500M Hz, $CDCl_3$, δ): 7.85 (d, J = 8.0 Hz, 2H), 7.75 (d, J = 7.0 Hz, 2H), 7.71 (s, 2H), 7.539 (t, J = 7.5 Hz, 2H); ^{13}C NMR (125M Hz, $CDCl_3$, δ): 193.52, 139.03, 132.99, 130.63, 129.07, 127.25, 125.28, 122.36; HRMS (FAB) (m/z): $[M+H]^+$ cal. for $C_{15}H_9O$: 205.0653, found: 205.0657.

Compound 4

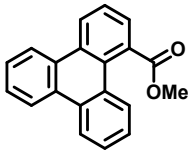

Methyl 2'-bromo-[1,1'-biphenyl]-2-carboxylate (1.96 g, 6.8 mmol), 2-(trimethylsilyl)phenyl trifluoromethanesulfonate (4 g, 13.4 mmol) and tri(o-tolyl)phosphine (0.1 g, 3.3 mmol) were placed in a 250 mL flask and dried under vacuum for one hour. Dried toluene (60 mL), dried acetonitrile (20 mL), tris(dibenzylideneacetone)dipalladium(0) (0.3 g, 3.2 mmol) and cesium fluoride (6.1 g, 40 mmol) were added in order under nitrogen. The mixture was refluxed under nitrogen overnight and cooled to room temperature when starting material was all consumed as indicated by TLC check. The solvent was removed and the crude was purified by column chromatography on silica gel column using hexane: dichloromethane (2:1) as the eluent to give the target product as white solid (0.9 g, 47%). ^{1}H NMR (500M Hz, $CDCl_3$, δ): 8.71 (d, J = 8.5 Hz, 1H), 8.61 -8.57 (m, 3H), 8.04 (d, J = 8.0 Hz, 1H), 7.80 (d, J = 7.0 Hz, 1H), 7.66 -7.63 (m, 4H), 7.52 (t, J = 7.0 Hz, 1H), 3.89 (s, 3H).; ^{13}C NMR (125M Hz, $CDCl_3$, δ): 172.62, 131.13, 131.03, 130.75, 130.15, 129.22, 128.68, 128.47, 128.43, 127.79, 127.72, 127.68, 127.54, 126.32, 126.13, 125.39, 123.39(2), 123.27, 52.61.; HRMS (FAB) (m/z): $[M]^+$ cal. for $C_{20}H_{14}O_2$: 286.0994 , found: 286.0994.

Compound 5

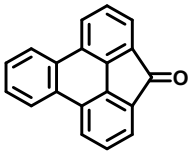

Compound **4** (2 g, 7 mmol) was hydrolyzed by 20% KOH in methanol solution (40 mL), then the solution was acidified by HCl to give triphenylene-1-carboxylic acid. To the acid solution was added Eaton's reagent (30 mL) and heated at 80℃ for 3 h. The mixture was poured to crushed ice, and yellow solid was obtained. The precipitates

were filtered and washed by water. The filtered cake was purified by recrystallization from methanol to give the target product (**5**) as pure yellow solid (1.68 g, 95%). ^{1}H NMR (500M Hz, $CDCl_3$, δ): 8.54 -8.52 (m, 2H), 8.55 (d, *J* = 8.0 Hz, 2H), 7.78 (d, *J* = 7.0 Hz, 2H), 7.73 -7.71 (m, 2H), 7.61 (t, *J* = 7.5 Hz, 2H).;^{13}C NMR (125M Hz, $CDCl_3$, δ): 193.75, 138.36, 132.77, 129.73, 129.39, 127.63, 127.38, 126.38, 124.22, 122.95.; HRMS (FAB) (m/z): $[M+H]^+$ cal. for $C_{19}H_{11}O$: 255.0810, found: 255.0813.

Compound 7

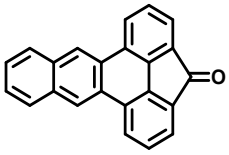

The compound **6** (2.5g, 8.6 mmol) was dissolved in anhydrous THF and cooled to -78℃. 2.5M n-BuLi (4.3 mL, 10.7 mmol) was added dropwise, then the solution was stirred at -78˚C for 1 h. The solution was purged with dry oxygen gas and slowly warmed up to room temperature for 3 h. The solvent was removed and the crude product was purified by washing with methanol, ethanol and diethyl ether. Yellow solid was obtained, yield = 80%, ^{1}H NMR (400M Hz, $CDCl_3$, δ): 8.79(s, 2H), 8.32 (d, *J* =8.0 Hz, 2H), 8.05-8.02 (m, 2H), 7.69 (d, *J*= 7.2 Hz, 2H), 7.62-7.59 (m, 2H), 7.51 (t, *J*= 7.2 Hz, 2H);^{13}C NMR (100M Hz, $CDCl_3$, δ): 193.63, 138.64, 132.63, 132.02, 129.47, 128.12, 127.80, 127.47, 126.77, 126.66, 123.23, 123.14; HRMS (FAB) (m/z): [M+H]+ cal. for $C_{23}H_{13}O$: 3050966, found: 305.0974.

(B) **NMR spectra**

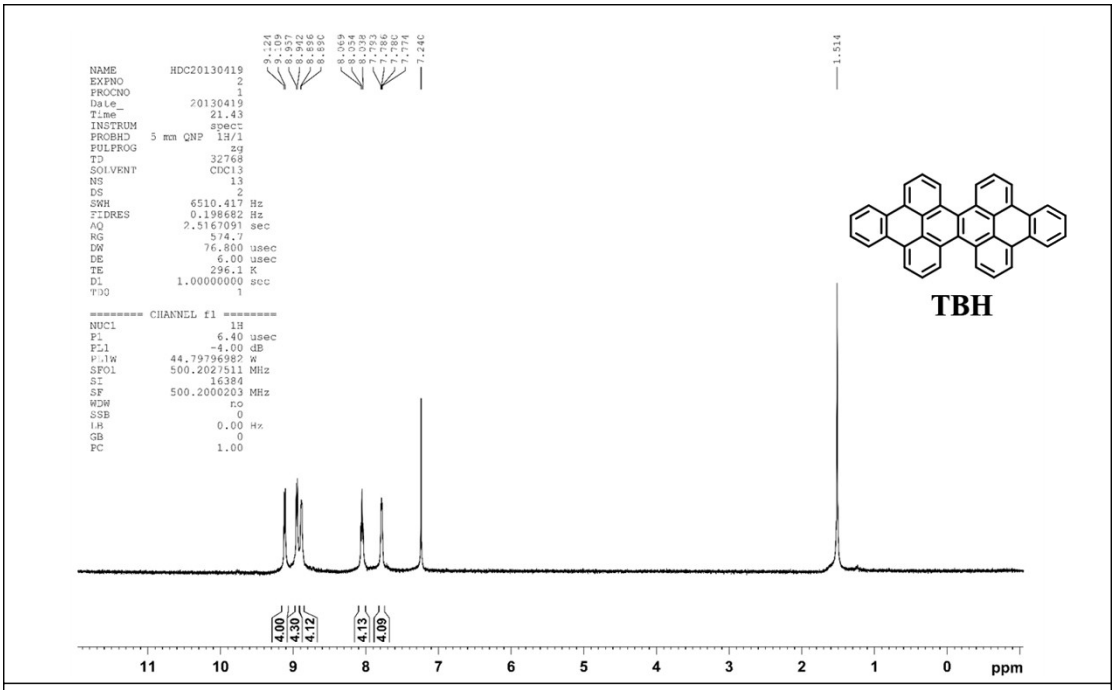

^{1}H-NMR of compound **TBH**

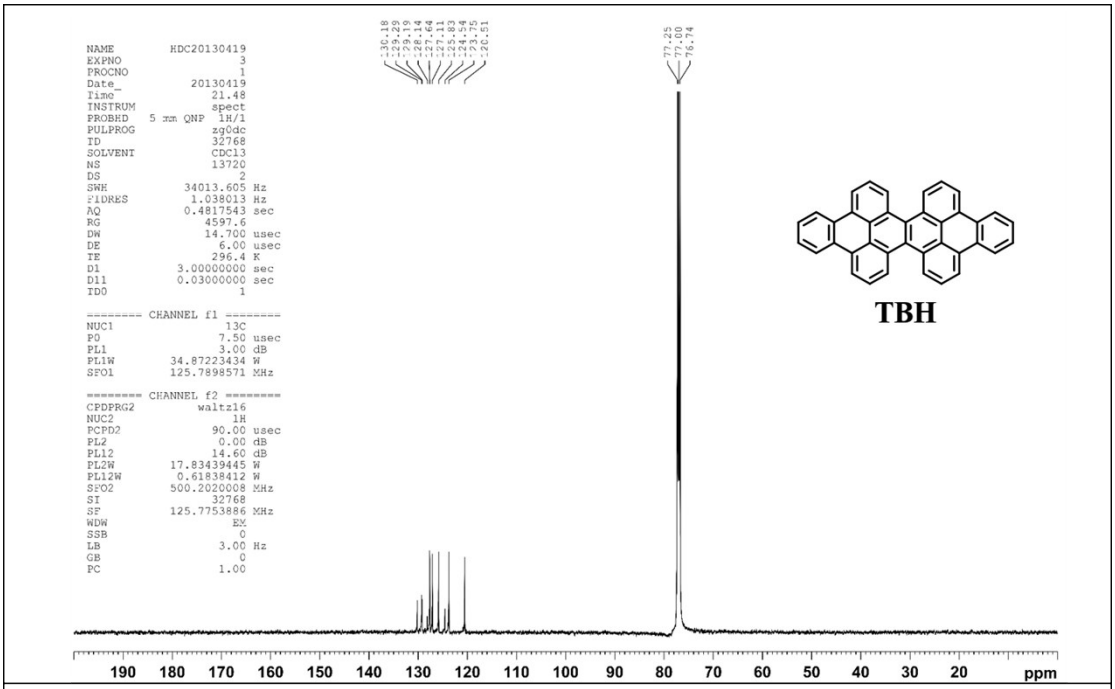

^{13}C-NMR of compound **TBH**

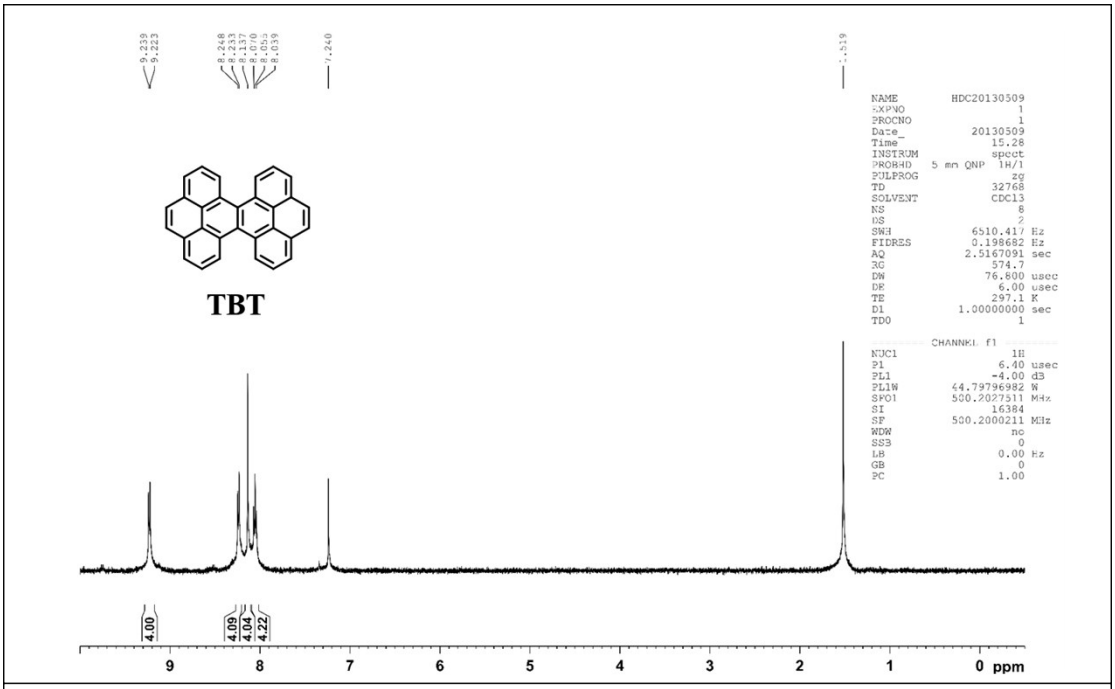

^{1}H-NMR of compound **TBT**

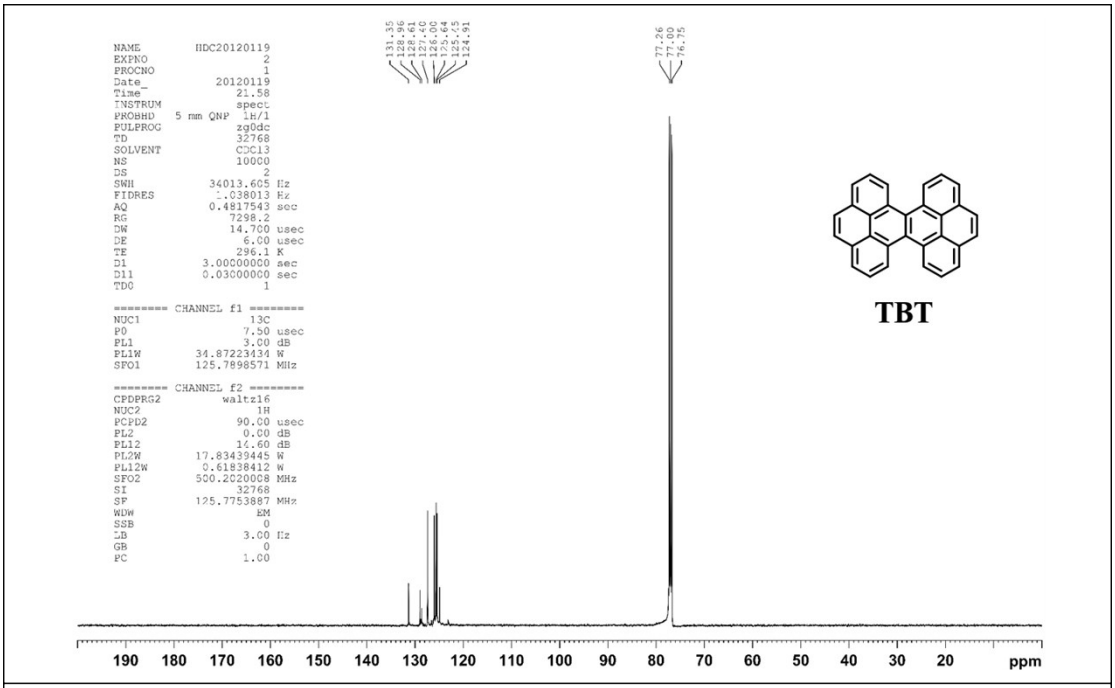

^{13}C-NMR of compound **TBT**

^{1}H-NMR of compound **TBH**

^{13}C-NMR of compound **TBH**

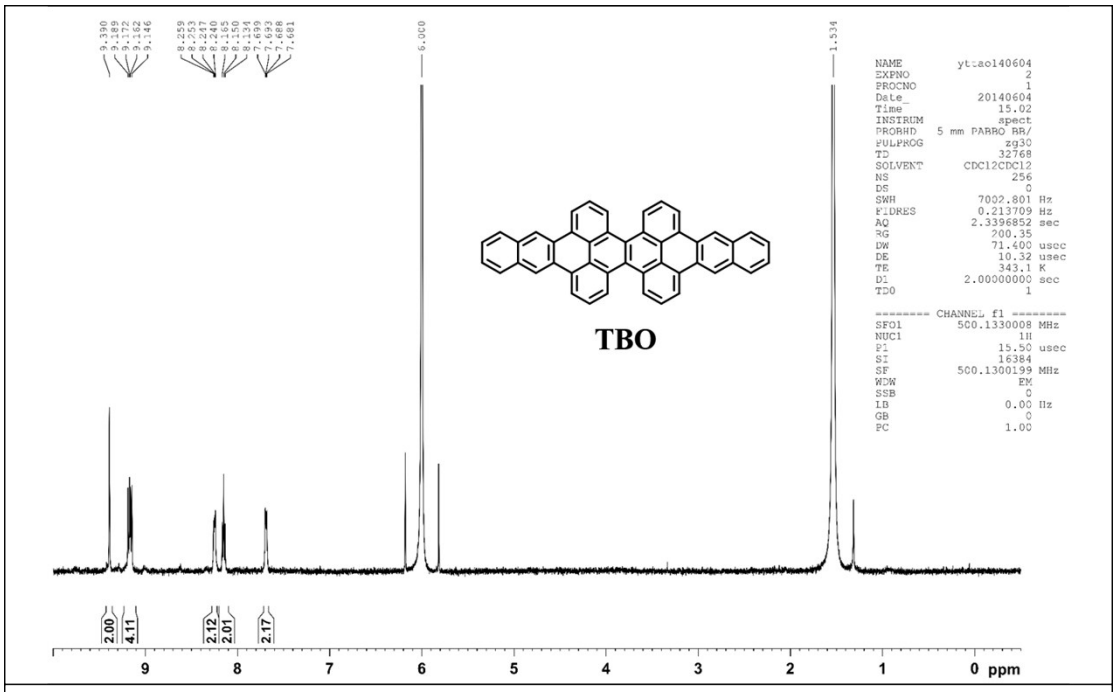

^{1}H-NMR of compound **TBO**

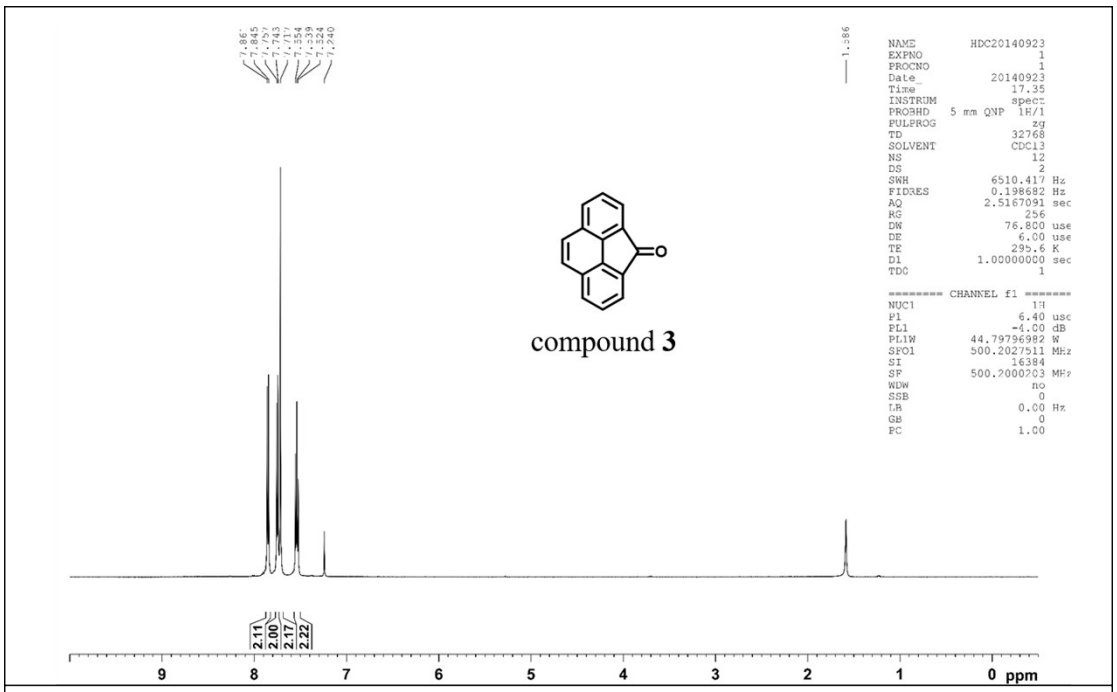

^{1}H-NMR of compound **3**

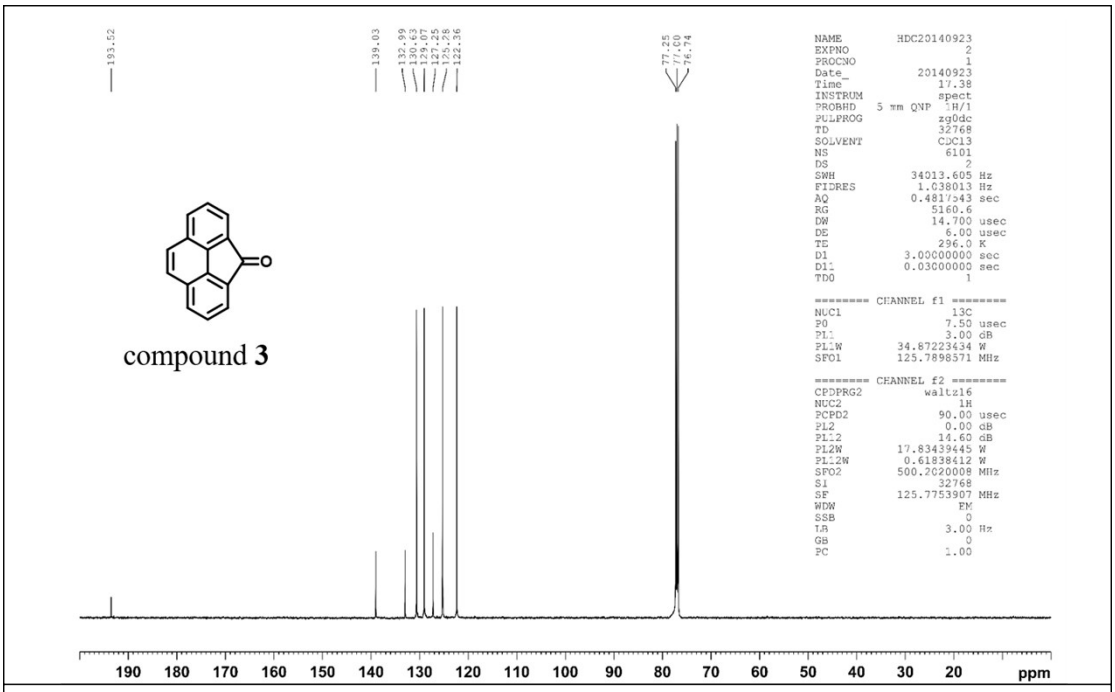

^{13}C-NMR of compound **3**

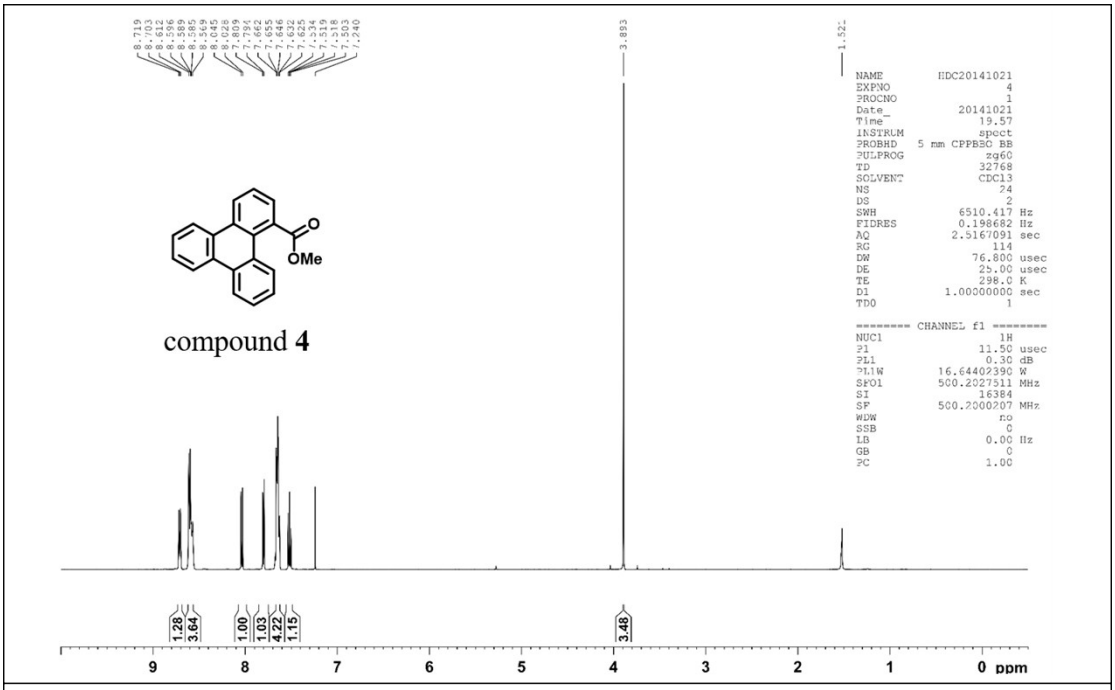

^{1}H-NMR of compound **4**

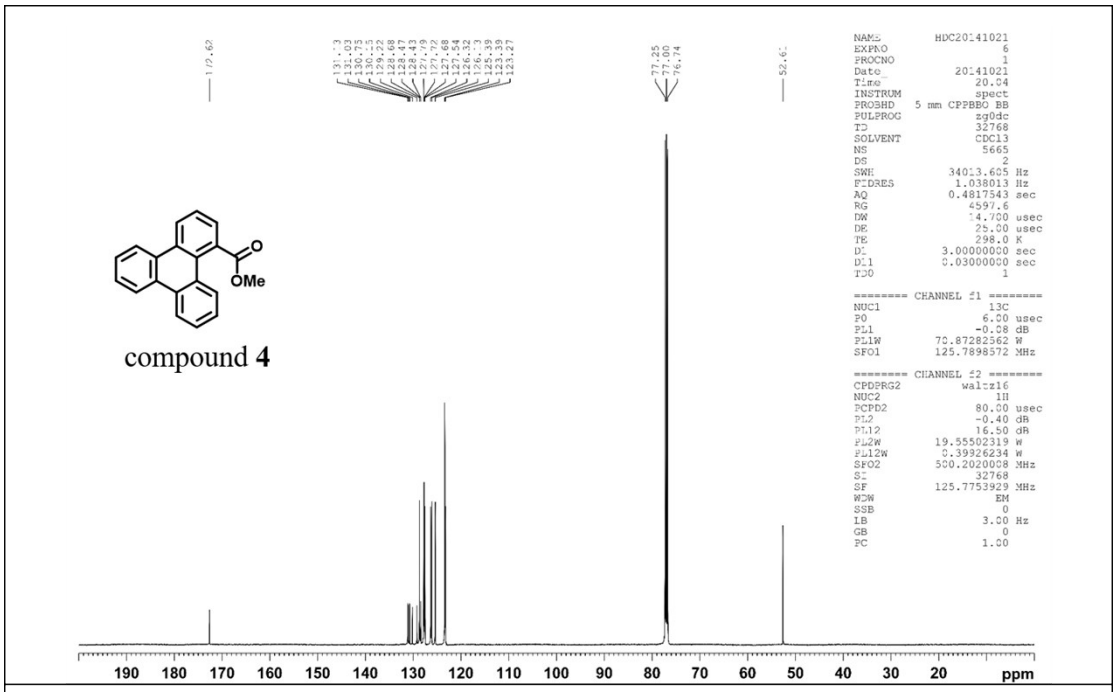

^{13}C-NMR of compound **4**

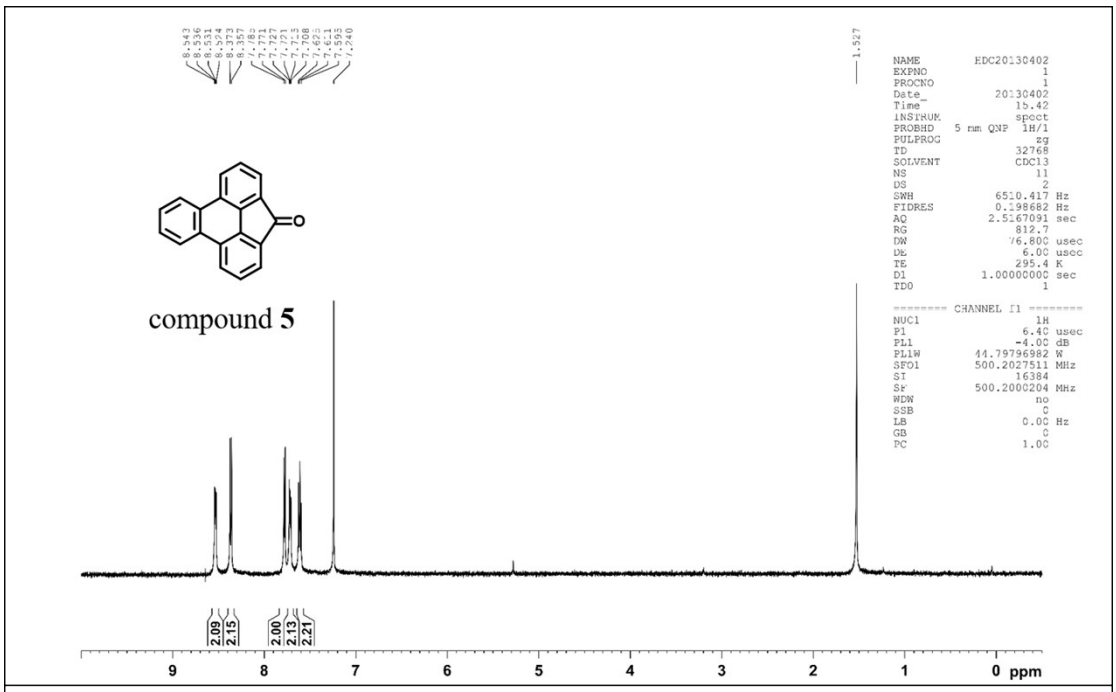

^{1}H-NMR of compound **5**

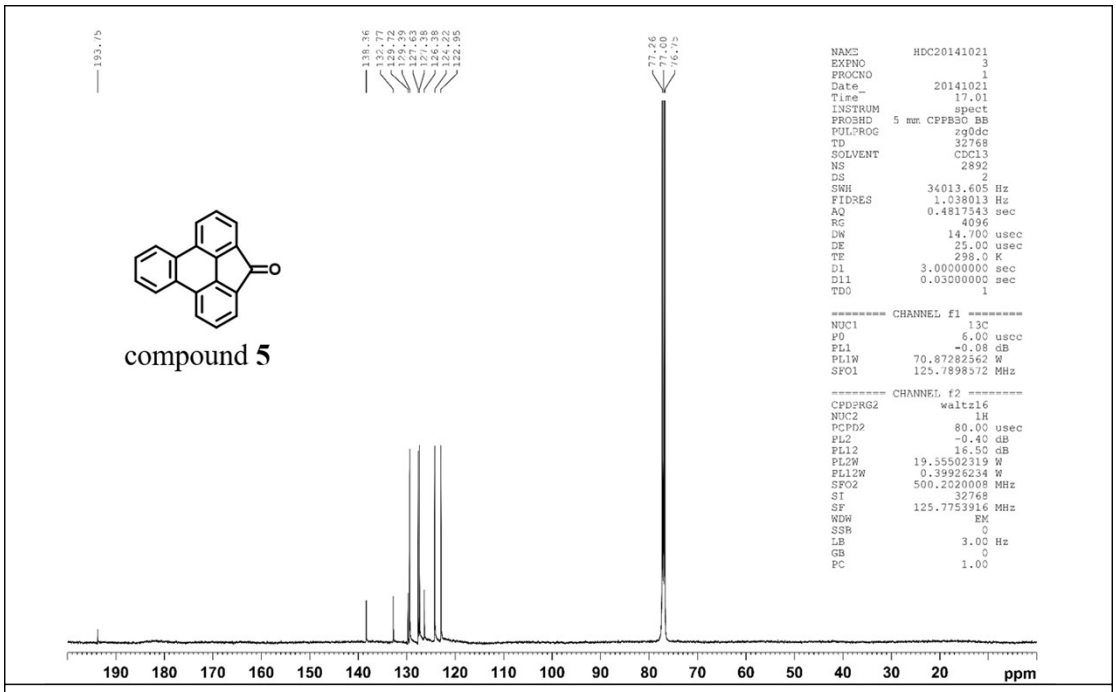

^{13}C-NMR of compound **5**

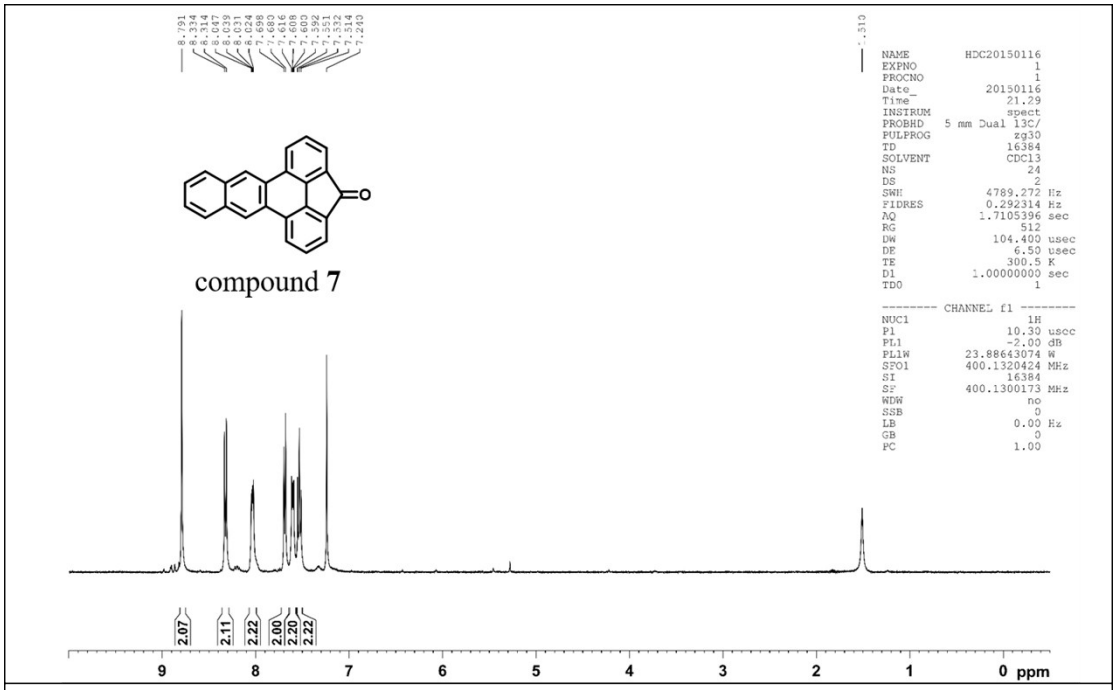

^{1}H-NMR of compound **7**

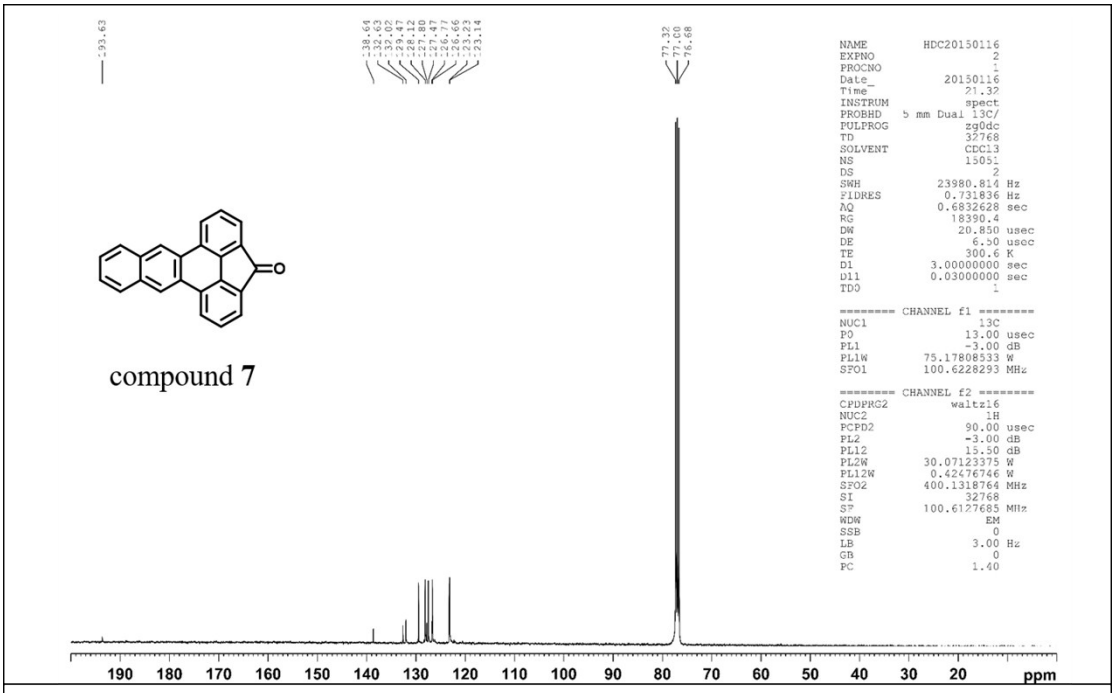

^{13}C-NMR of compound **7**

(C) Computational details

Density functional theory computation was used for determining the structures and the energies of molecules. The neutral and cationic calculations are with the (U)B3LYP functional and 6-31G* basis set.[1,2] The optimized structures are listed in Tables S4, S6, S8, and S10. The inner reorganization energy (λ_{in}) is calculated with the four-point method:[3,4]

$$\lambda_{in} = \left(E(N,C_{opt}) - E(N,N_{opt})\right) + \left(E(C,N_{opt}) - E(C,C_{opt})\right),$$

where $E(A,B)$ is the energy obtained form state A at coordinate B, and N_{opt}(C_{opt}) is the optimized structure of the neutral (cationic) molecule.

The electronic coupling (V) for the charge hopping process was evaluated by the direct coupling (DC) scheme.[5] The electronic coupling values were calculated by the LC-ωPBE[6,7] scheme (ω = 0.2) and the Dunning's double-ζ basis sets (DZP)[8]. In DC calculations, we first obtained two charge-localized states for the reactant state Ψ_r and the product state Ψ_p. The electronic coupling was then evaluated by

$$V = \frac{H_{rp} - (E_r + E_p)/2}{1 - S_{rp}^2},$$

where E_r and E_p are the energies for the reactant state and the product state, and H_{rp} and S_{rp} are the off-diagonal matrix elements for the Hamiltonian and the overlap matrix, respectively. All the quantum chemistry calculations were performed with a developmental version of Q-Chem.[9] The dimer configurations were obtained from the crystal structure, with the hydrogen coordinates optimized at the level of B3LYP/6-31G*. The calculated values are listed in **Tables S5, S7, S9, and S11.**

To see the thermal fluctuation of the electronic coupling, we also sample the configurations from molecular dynamics (**MD**) simulations in the canonical ensemble (**NVT**) at 298 K. The **MD** simulation was performed using the Tinker program with the MM3 force field.[10-12] The supercell was formed based on the crystal unit cell with the sizes as listed in **Table S1**. The simulation time step was 1 fs. The trajectories were recorded with time interval of 0.1 ps. We sampled the dimer configurations with neighbors of a central molecule after equilibrating the system for 100 ps. The distributions of coupling strengths, together with a multi-Gaussian fitting, are included in **Figures S3**, **S6**, **S9** and **S12**. We note that the signs of the coupling is determined according to our computational results, as listed in Tables S5, S7, S9, S11, even though the absolute values are shown in the figures.

Based on the Einstein relation, the charge mobility (μ_E) can be estimated from the diffusion coefficient:[13,14]

$$\mu_E = \frac{e}{k_B T} D,$$

where e is the electronic charge, k_B is the Boltzmann constant, T is temperature and D is the diffusion coefficient. The diffusion coefficient can be calculated as

$$D \approx \frac{1}{2n} \sum_i r_i^2 k_i P_i ,$$

where n is the spatial dimensionality (1 in this calculation)[14], r_i is the projection of the hopping pathway on the direction of electric field for pathway i, k_i is the hopping rate and P_i is the hopping probability, which is proportional to the hopping rate:

$$P_i = \frac{k_i}{\sum_i k_i} ,$$

and the k_i can be evaluated by Marcus equation:

$$k_i = \frac{V^2}{\hbar} \sqrt{\frac{\pi}{4 \lambda k_B T}} \exp\left[\frac{-\lambda}{4 k_B T}\right],$$

where λ is the reorganization of the compound. The μ_E reported in the maintext were calculated with fixed coupling values derived from crystal structure.

Kinetic Monte Carlo (KMC) simulation was carried out on the lattice of 9600 molecules under the periodic boundary condition.[15] The number of unit cells in axis, for different molecules, are included in **Table S2**. The charge mobility is calculated by

$$\mu_{KMC} = \frac{\vec{d}}{t \cdot \vec{E}},$$

where $\vec{d}$ is the drift distance of charge carrier after one million hopping steps, t is the total drift time and $\vec{E}$ is the applied electric field, which is 10^5 V/cm in the simulation. The hopping time for each step is calculated as

$$t_s = \frac{r}{\sum_i k_i} ,$$

where k_i is the rate for the hopping process to the neighbor site i and the r is a random number following an exponential distribution $\exp(-r)$. The total drift time t is the sum of all t_s. For charge at each site, there are several possible hopping paths. The probability for each hopping path is proportional to their corresponding hopping rates

$$P_i = \frac{k_i}{\sum_i k_i} ,$$

where the inter-site hopping rate is calculated by the Marcus theory:

$$k_i = \frac{V^2}{\hbar}\sqrt{\frac{\pi}{4\lambda k_B T}}\exp\left[\frac{-(\Delta G+\lambda)^2}{4\lambda k_B T}\right].$$

The electronic coupling (V) is randomly generated by the coupling distributions obtained *via* the MD simulations, as shown in **Figures S3**, **S6**, **S9** and **S12**. The Free energy ΔG is calculated by

$$\Delta G = q\underset{r_i}{\rightharpoonup}\cdot\underset{E}{\rightharpoonup} + \Delta\varepsilon,$$

where q is charge, $\vec{r_i}$ is the vector of hopping pathway, $\vec{E}$ is the electric field, and Δε is energy change from the site energy ($\varepsilon_f - \varepsilon_i$). To simulate the system with disorder, the site energies ε_i and ε_f are randomly determined with a normal distribution ρ(ε) with standard derivation of 1 k_BT,

$$\rho(\varepsilon) = \frac{1}{\sqrt{2\pi\sigma^2}}\exp\left[-\frac{\varepsilon^2}{2\sigma^2}\right].$$

When the intersite coupling is larger than the reorganization energy by 1 k_BT, we assume the charge is delocalized among these sites, forming a charge delocalized domain *D*. Therefore, we employed a delocalized model for the polaron.[16] The delocalized state (ψ_i) is obtained by the linear recombination of the localized state ($|a\rangle$)

$$|\psi_i\rangle = \sum_{a\in D} c_{ia}|a\rangle,$$

which is the eigenstate of the Hamiltonian for the delocalized polaron:

$$H = \sum_{a\in D}\varepsilon_a|a\rangle\langle a| + \sum_{a,b\in D, a>b}(V_{ab}|a\rangle\langle b| + h.c.),$$

and the corresponding eigenvalue is ε_i. In the Hamiltonian, *h.c.* stands for Hermition conjugate. In simulation, the diagonal single-site energies ε_a was sampled from a normal distribution with standard derivation of 1 k_BT, and the coupling V_{ab} was sampled with the distribution obtained from MD simulation.

The hopping rate between the delocalized states ψ_i and ψ_f is

$$k_{if} = \frac{2\pi}{\hbar}|V_{if}|^2\frac{1}{\sqrt{4\pi\lambda_{if}k_BT}}exp\left[-\frac{(\lambda_{if}+\Delta G_{if})^2}{4\lambda_{if}k_BT}\right].$$

The electronic coupling V_{if} is

$$V_{if} = \langle\psi_i|H|\psi_f\rangle = \sum_a\sum_b c_{ia}c_{fb}V_{ab},$$

where the V_{ab} is the intersite coupling between site a and site b

$V_{ab} = \langle a|H|b\rangle$.

The change of free energy ΔG_{if} is

$$\Delta G_{if} = q\vec{r}_{if} \cdot \vec{E} + \varepsilon_f - \varepsilon_i ,$$

where the ε_i (ε_f) are the eigenenergy of delocalized state i (f), $\vec{r}_{if}$ is the hopping distance given by

$$\vec{r}_{if} = \vec{r}_f - \vec{r}_i ,$$

where the $\vec{r}_j$ is the location of the state ψ_j, estimated by an weighted averaged value with the probability of the charge at the site $|c_{ja}|^2$ as the weighting factor:

$$r_j = \sum_{a \in D} |c_{ja}|^2 r_a .$$

The reorganization energy λ for the delocalized polaron is given by an averaged value of the initial and final state, with each λ calculated from as a weighted average of each molecule, with $|c_{ia}|^4$ as the weighting factor which accounts for the participation ratio.[16]

$$\lambda_{if} = \frac{1}{2}(\lambda_i + \lambda_f) = \frac{\lambda}{2}\left[\sum_{a \in D_i} |c_{ia}|^4 + \sum_{b \in D_f} |c_{fb}|^4\right] ,$$

where D_i and D_f are the domains for the initial and final states, or the range of the donor and acceptor polarons, respectively. The site energy ε_a and coupling V_{ab} were randomly generated. In our work we have generated 100 such disordered Hamiltonians. The charge mobility (μ_{KMC}) was evaluated by an averaged value of one thousand simulating results, with 10 trajectories obtained from each of the 100 randomly generated Hamiltonians.

· **Table S1**. Periodic box size for molecular dynamic simulation

Compound	*a*	*b*	*c*	n*a*	n*b*	n*c*
TBH	18.8657	7.6482	31.436	2	4	2
TBN	12.1404	7.5623	17.6416	4	2	2
TBO	31.9402	3.8977	23.9483	2	4	2
TBT	13.1759	7.4913	18.1519	4	2	2

· **Table S2**. Periodic box size for Monte Carlo simulation

Compound	n*a*	n*b*	n*c*	Site
TBH	10	12	10	9600

TBN	10	24	10	9600
TBO	10	24	10	9600
TBT	10	24	10	9600

· **Table S3.** Simulated charge mobilities of tetrabenzoacene derivatives (in the units of cm2 V-1 s-1)

Simulated mobility	**TBN**	**TBT**	**TBH**	**TBO**
μ_{KMC}	0.72 (0.0005) [a)]	2.24 (0.0018)	1.24 (0.0007)	5.64 (0.0083)
μ_{deloc}	0.72 (0.0005)	0.45 (0.0019)	1.24 (0.0007)	0.35 (0.0075)

[a] In parentheses are standard deviation for the Monte Carlo statistics.

· **Computational results of TBN**

· **Table S4**. Optimized structures of **TBN**

	Optimized neutral structure			Optimized cationic structure		
	X	Y	Z	X	Y	Z
C	1.20628	-1.42972	0.31173	1.22847	-1.39103	0.34913
C	1.17595	-2.73958	0.85041	1.22057	-2.69822	0.90241
C	2.33237	-3.39368	1.23838	2.39511	-3.31361	1.30392
C	3.57369	-2.75399	1.11474	3.61033	-2.63196	1.17625
C	3.62803	-1.45680	0.63552	3.63834	-1.33174	0.67342
C	2.46403	-0.76641	0.23576	2.46650	-0.68437	0.26226
C	2.50570	0.61097	-0.23941	2.46646	0.68458	-0.26204
C	3.70853	1.22763	-0.64488	3.63828	1.33198	-0.67321
C	3.73305	2.52622	-1.12270	3.61021	2.63217	-1.17613
C	2.53383	3.24284	-1.24020	2.39496	3.31373	-1.30391
C	1.34075	2.66189	-0.84701	1.22044	2.69829	-0.90240
C	1.29197	1.35220	-0.30906	1.22839	1.39115	-0.34898
C	0.02245	0.69851	0.00317	-0.00004	0.71842	0.00009
C	-1.20345	1.43122	0.31314	-1.22851	1.39107	0.34914
C	-1.17041	2.74286	0.84752	-1.22064	2.69822	0.90253
C	-2.32488	3.39860	1.23822	-2.39521	3.31362	1.30396
C	-3.56699	2.75897	1.12164	-3.61043	2.63201	1.17611
C	-3.62377	1.46025	0.64707	-3.63842	1.33182	0.67322
C	-2.46164	0.76788	0.24504	-2.46654	0.68443	0.26217
C	-2.50560	-0.61121	-0.22471	-2.46649	-0.68455	-0.26206
C	-3.71059	-1.22988	-0.62078	-3.63830	-1.33205	-0.67311
C	-3.73752	-2.53019	-1.09361	-3.61019	-2.63228	-1.17591
C	-2.53872	-3.24684	-1.21580	-2.39492	-3.31382	-1.30365
C	-1.34363	-2.66413	-0.83160	-1.22041	-2.69832	-0.90222
C	-1.29215	-1.35253	-0.29842	-1.22840	-1.39111	-0.34896
C	-0.02117	-0.69794	0.00525	0.00001	-0.71835	0.00008
H	0.22087	-3.22263	1.01557	0.27403	-3.19682	1.07250
H	2.26998	-4.39205	1.66289	2.36583	-4.30585	1.74249
H	4.48518	-3.25767	1.42465	4.53508	-3.10104	1.49816
H	4.58657	-0.95000	0.60294	4.58883	-0.81224	0.62999
H	4.63392	0.66223	-0.61814	4.58880	0.81253	-0.62973
H	4.67301	2.97193	-1.43645	4.53494	3.10128	-1.49805
H	2.53227	4.24318	-1.66454	2.36563	4.30592	-1.74258

H	0.41628	3.20278	-1.00668	0.27388	3.19680	-1.07262
H	-0.21439	3.22599	1.00704	-0.27411	3.19677	1.07279
H	-2.26045	4.39827	1.65935	-2.36595	4.30582	1.74262
H	-4.47706	3.26415	1.43329	-4.53520	3.10110	1.49793
H	-4.58275	0.95398	0.61984	-4.58892	0.81235	0.62968
H	-4.63612	-0.66490	-0.59045	-4.58884	-0.81265	-0.62963
H	-4.67923	-2.97742	-1.39983	-4.53492	-3.10146	-1.49772
H	-2.53931	-4.24862	-1.63673	-2.36557	-4.30606	-1.74221
H	-0.41986	-3.20517	-0.99477	-0.27384	-3.19682	-1.07235

· **Table S5.** Distance and electronic coupling of charge hopping path in **TBN**

Type	Distance (Å)	Coupling (meV)
I	12.140	-0.75
II	4.815	-75.64
III	9.931	1.56
IV	10.207	-11.91
V	10.249	28.72
VI	8.893	-1.57
VII	10.159	1.76
VIII	11.472	-7.84

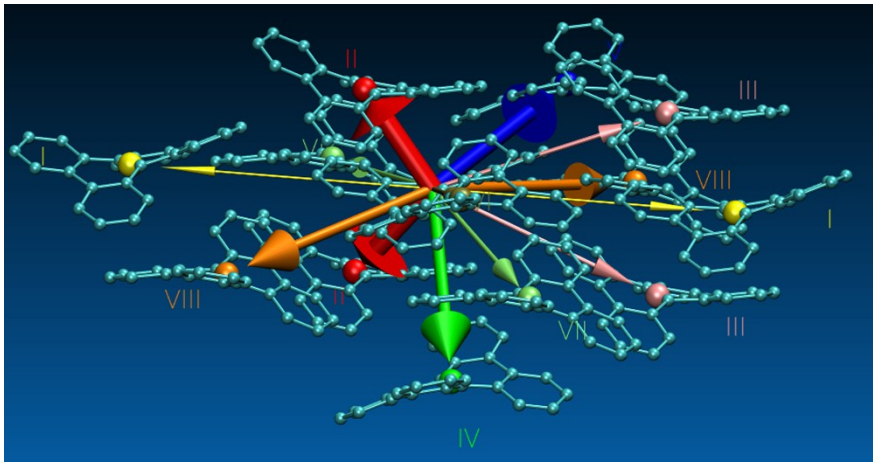

Figure S1. Charge hopping paths of **TBN**.

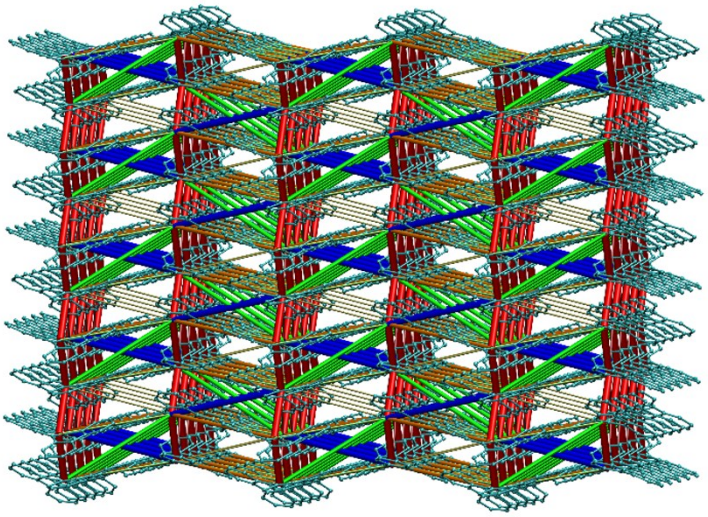

Figure S2. Charge hopping paths in **TBN** lattice

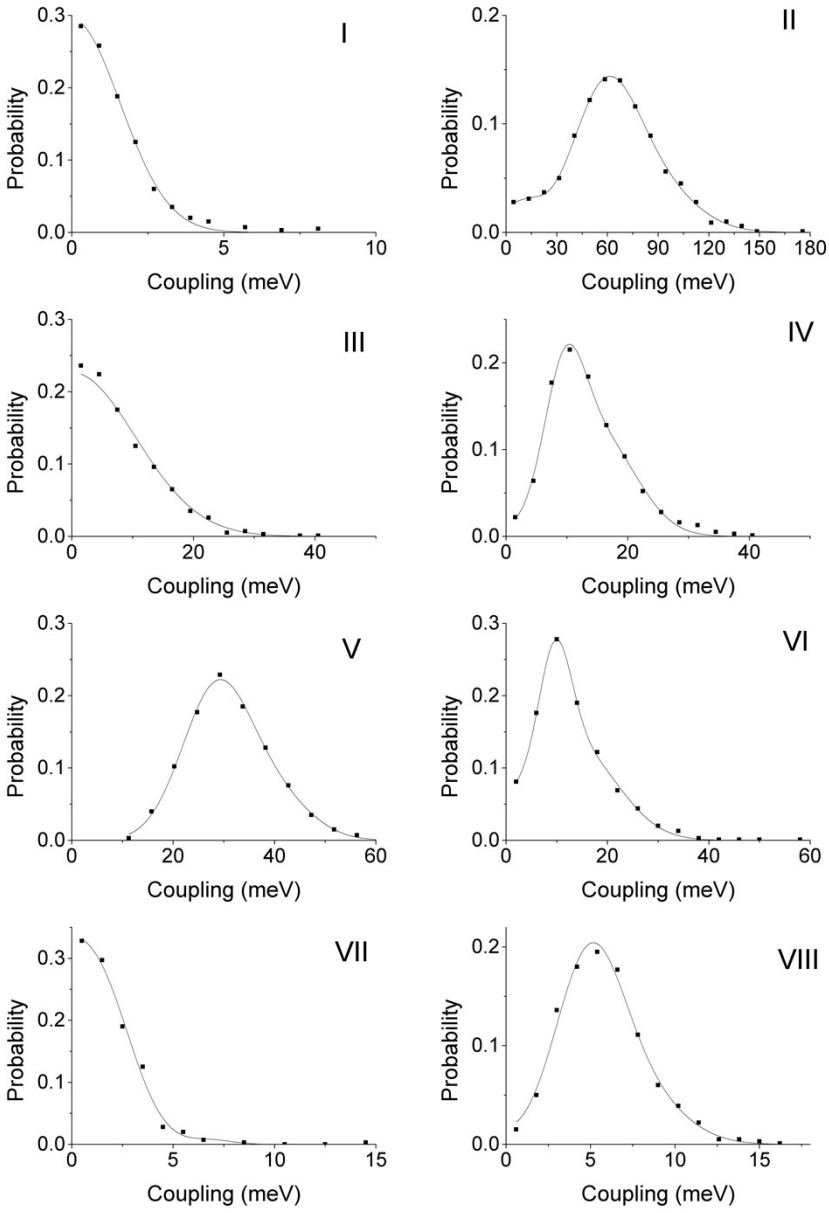

Figure S3. Distributions of the electronic coupling for the charge hopping paths in **TBN**.

· **Computational results of TBT**

· **Table S6**. Optimized structures of **TBT**

	Optimized neutral structure			Optimized cationic structure		
	X	Y	Z	X	Y	Z
C	1.29304	-2.72899	0.75935	1.27938	-2.72297	0.79157
H	0.36940	-3.25333	0.96767	0.35402	-3.23333	1.02911
C	2.50293	-3.36769	1.03475	2.49187	-3.36564	1.05218
H	2.49222	-4.38546	1.41543	2.48814	-4.37995	1.43827
C	3.71073	-2.71604	0.82560	3.69307	-2.70664	0.83606
H	4.65379	-3.22600	1.00633	4.63695	-3.21233	1.02015
C	4.95379	-0.66450	0.19957	4.93334	-0.65252	0.20555
H	5.88865	-1.19397	0.36730	5.87024	-1.17662	0.37148
C	4.95696	0.63238	-0.20933	4.93334	0.65228	-0.20565
H	5.89438	1.15642	-0.37980	5.87024	1.17637	-0.37160
C	3.72405	2.69128	-0.83134	3.69307	2.70649	-0.83589
H	4.66952	3.19577	-1.01481	4.63695	3.21219	-1.01997
C	2.51947	3.35005	-1.03671	2.49187	3.36557	-1.05176
H	2.51361	4.36801	-1.41699	2.48814	4.37996	-1.43765
C	1.30667	2.71839	-0.75792	1.27939	2.72291	-0.79113
H	0.38552	3.24821	-0.96330	0.35400	3.23336	-1.02841
C	-1.29025	2.72436	0.76812	-1.27926	2.72297	0.79121
H	-0.36598	3.24825	0.97472	-0.35384	3.23338	1.02848
C	-2.49931	3.36262	1.04818	-2.49171	3.36569	1.05184
H	-2.48745	4.37975	1.43054	-2.48792	4.38008	1.43773
C	-3.70774	2.71138	0.84145	-3.69294	2.70667	0.83597
H	-4.65026	3.22106	1.02572	-4.63680	3.21241	1.02005
C	-4.95267	0.66092	0.21562	-4.93331	0.65252	0.20573
H	-5.88703	1.19007	0.38709	-5.87018	1.17666	0.37168
C	-4.95707	-0.63525	-0.19554	-4.93337	-0.65228	-0.20547
H	-5.89500	-1.15899	-0.36411	-5.87029	-1.17634	-0.37140
C	-3.72604	-2.69301	-0.82505	-3.69320	-2.70646	-0.83598
H	-4.67207	-3.19715	-1.00658	-4.63711	-3.21211	-1.02007
C	-2.52210	-3.35138	-1.03533	-2.49203	-3.36552	-1.05209
H	-2.51739	-4.36863	-1.41753	-2.48835	-4.37983	-1.43818
C	-1.30844	-2.72023	-0.75906	-1.27951	-2.72291	-0.79149
H	-0.38794	-3.24964	-0.96834	-0.35418	-3.23332	-1.02903
C	3.72405	-1.37671	0.40484	3.70800	-1.35744	0.41215

C	3.73080	1.35178	-0.41093	3.70801	1.35724	-0.41214
C	2.48633	-0.70134	0.17266	2.47233	-0.68769	0.18445
C	2.48982	0.68364	-0.17526	2.47234	0.68748	-0.18444
C	1.25027	-1.40880	0.27395	1.24009	-1.40064	0.29606
C	1.25759	1.39832	-0.27278	1.24012	1.40047	-0.29592
C	-0.00178	-0.70182	0.00174	-0.00002	-0.71452	0.00004
C	0.00229	0.69857	0.00303	0.00002	0.71437	0.00004
C	-1.25790	-1.40107	-0.27163	-1.24016	-1.40058	-0.29598
C	-1.24894	1.40505	0.28024	-1.24005	1.40053	0.29599
C	-2.48983	-0.68658	-0.16905	-2.47237	-0.68757	-0.18437
C	-2.48531	0.69779	0.18133	-2.47231	0.68760	0.18451
C	-3.73152	-1.35428	-0.40217	-3.70807	-1.35726	-0.41207
C	-3.72233	1.37276	0.41843	-3.70794	1.35742	0.41222

Table S7. Distance and electronic coupling of charge hopping path in **TBT**

Type	Distance (Å)	Coupling (meV)
I	13.176	0.455
II	11.296	0.378
III	4.927	-84.0
IV	8.152	38.8
V	12.518	-1.527
VI	8.579	16.91
VII	13.503	3.441
VIII	10.159	5.25
IX	12.198	5.095

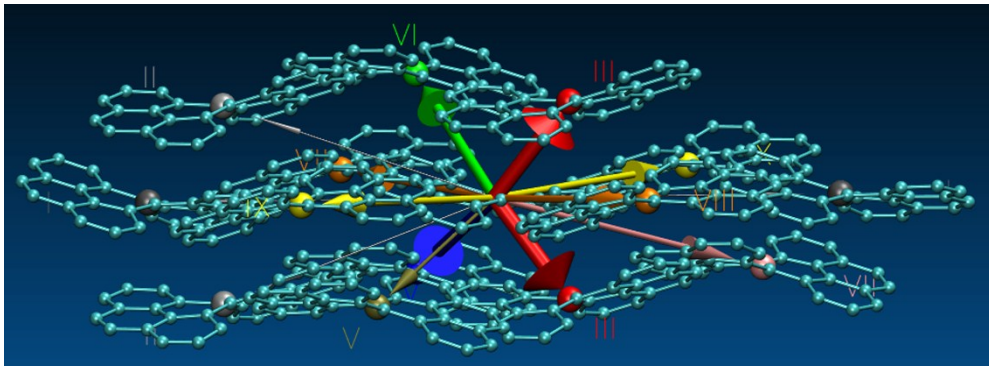

Figure S4. Charge hopping paths of **TBT**.

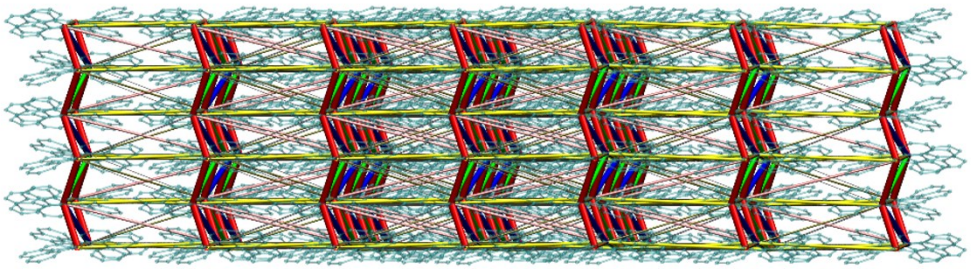

Figure S5. Charge hopping paths in **TBT** lattice.

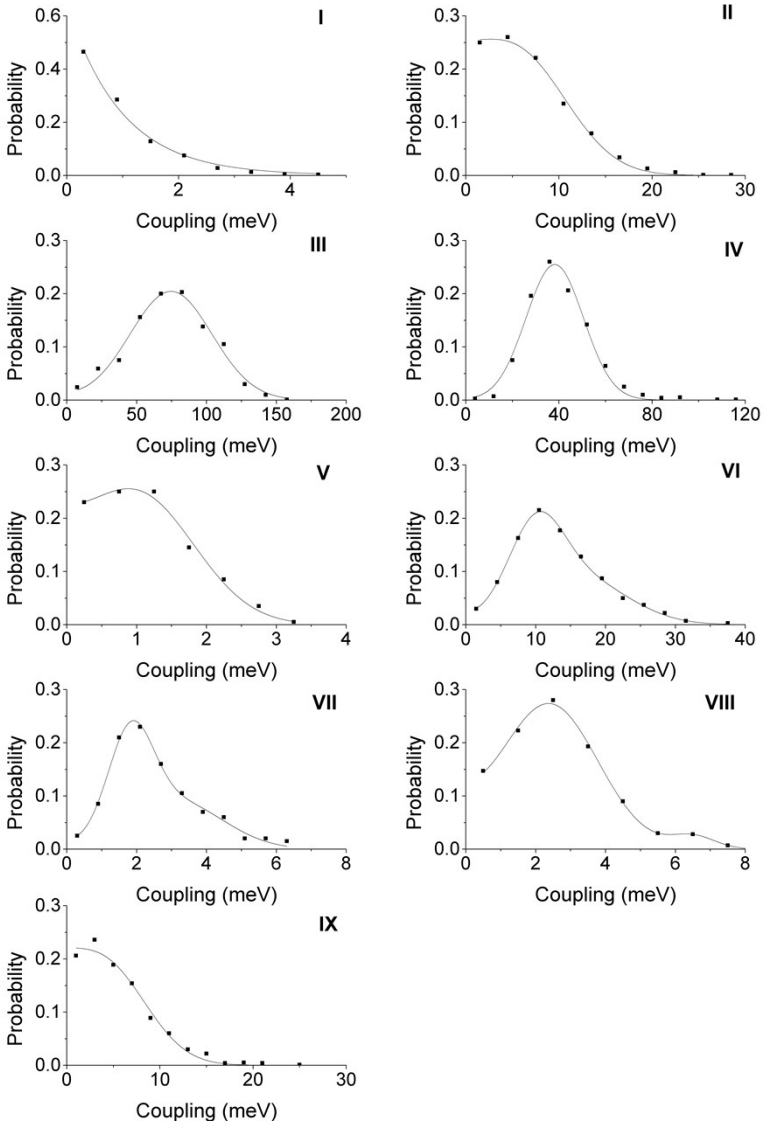

Figure S6. Distributions of the electronic coupling for the charge hopping path in **TBT**.

· **Computational results of TBH**

· **Table S8.** Optimized structures of **TBH**

	Optimized neutral structure			Optimized cationic structure		
	X	Y	Z	X	Y	Z
C	5.00135	0.61299	0.20424	4.97077	0.66795	0.23347
C	6.25107	1.23607	0.41872	6.21273	1.30469	0.45797
H	6.29080	2.25489	0.78567	6.24536	2.32600	0.81699
C	7.44465	0.58369	0.16703	7.40973	0.65470	0.22756
H	8.38835	1.09338	0.34103	8.34856	1.16916	0.40845
C	7.42707	-0.73145	-0.31598	7.40799	-0.66885	-0.24084
H	8.35699	-1.25447	-0.52177	8.34546	-1.18474	-0.42467
C	6.21635	-1.36524	-0.53012	6.20927	-1.31688	-0.46778
H	6.22867	-2.38194	-0.90471	6.23916	-2.33802	-0.82754
C	4.98372	-0.72384	-0.27447	4.96902	-0.67817	-0.23947
C	3.70471	-1.41396	-0.47225	3.70060	-1.36605	-0.45788
C	3.64043	-2.74232	-0.91631	3.64442	-2.70141	-0.91580
H	4.54703	-3.29361	-1.13427	4.55801	-3.23879	-1.13629
C	2.41744	-3.37386	-1.10987	2.43412	-3.34709	-1.13020
H	2.38855	-4.38393	-1.50945	2.42206	-4.35124	-1.54190
C	1.23134	-2.72445	-0.79538	1.23795	-2.70477	-0.83288
H	0.28985	-3.22282	-0.98700	0.29892	-3.19487	-1.05814
C	1.23553	-1.41182	-0.28751	1.23553	-1.39234	-0.31153
C	2.48613	-0.72550	-0.19976	2.47746	-0.69190	-0.20154
C	2.50336	0.66195	0.17937	2.47916	0.68644	0.20023
C	3.73968	1.32382	0.43798	3.70405	1.35797	0.45523
C	3.70827	2.64733	0.89977	3.65113	2.69287	0.91490
H	4.62868	3.17600	1.11611	4.56607	3.22798	1.13533
C	2.50104	3.30157	1.11647	2.44242	3.34081	1.13143
H	2.49808	4.30654	1.52966	2.43290	4.34446	1.54442
C	1.29804	2.68153	0.80661	1.24458	2.70140	0.83449
H	0.36902	3.19737	1.01243	0.30679	3.19327	1.06104
C	1.26922	1.37418	0.28625	1.23888	1.38947	0.31200
C	0.00882	0.69255	-0.00037	0.00082	0.71064	0.00032
C	-0.00740	-0.69998	0.00156	-0.00082	-0.71056	0.00033
C	-1.26789	-1.38075	0.28993	-1.23888	-1.38939	0.31201
C	-1.29692	-2.68679	0.81354	-1.24456	-2.70134	0.83448
H	-0.36802	-3.20226	1.02077	-0.30675	-3.19321	1.06100

C	-2.50003	-3.30601	1.12468	-2.44239	-3.34075	1.13146
H	-2.49722	-4.31008	1.54004	-2.43287	-4.34439	1.54445
C	-3.70717	-2.65211	0.90647	-3.65111	-2.69281	0.91495
H	-4.62768	-3.18025	1.12365	-4.56604	-3.22791	1.13541
C	-3.73835	-1.32961	0.44183	-3.70403	-1.35791	0.45526
C	-2.50197	-0.66865	0.18124	-2.47916	-0.68638	0.20025
C	-2.48465	0.71768	-0.20196	-2.47747	0.69196	-0.20154
C	-1.23402	1.40363	-0.29172	-1.23554	1.39240	-0.31156
C	-1.22958	2.71463	-0.80374	-1.23798	2.70481	-0.83297
H	-0.28801	3.21239	-0.99652	-0.29896	3.19490	-1.05830
C	-2.41555	3.36298	-1.12089	-2.43415	3.34712	-1.13028
H	-2.38652	4.37166	-1.52393	-2.42210	4.35126	-1.54201
C	-3.63863	2.73212	-0.92563	-3.64444	2.70145	-0.91583
H	-4.54511	3.28262	-1.14601	-4.55803	3.23883	-1.13630
C	-3.70316	1.40534	-0.47685	-3.70062	1.36609	-0.45788
C	-4.98226	0.71616	-0.27617	-4.96904	0.67819	-0.23947
C	-4.99993	-0.61903	0.20707	-4.97076	-0.66793	0.23348
C	-6.24963	-1.24083	0.42524	-6.21269	-1.30473	0.45794
H	-6.28933	-2.25814	0.79638	-6.24528	-2.32605	0.81694
C	-7.44323	-0.58895	0.17234	-7.40971	-0.65478	0.22751
H	-8.38694	-1.09762	0.34931	-8.34852	-1.16928	0.40838
C	-7.42566	0.72437	-0.31557	-7.40801	0.66877	-0.24088
H	-8.35560	1.24695	-0.52236	-8.34550	1.18463	-0.42472
C	-6.21493	1.35703	-0.53304	-6.20932	1.31685	-0.46780
H	-6.22727	2.37245	-0.91109	-6.23924	2.33798	-0.82757

· **Table S9.** Distance and electronic coupling of charge hopping path in **TBH**

Type	Distance (Å)	Coupling (meV)
I	7.648	-29.276
II	10.116	4.204
III	12.261	2.302
IV	6.491	41.438
V	10.553	50.570
VI	9.374	-13.201

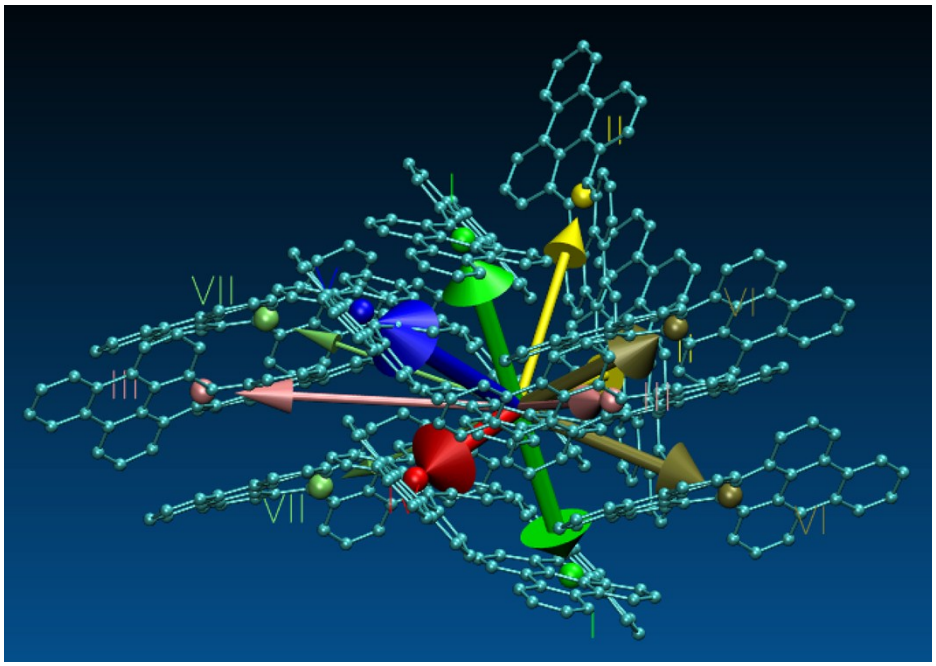

Figure S7. Charge hopping paths of **TBH**.

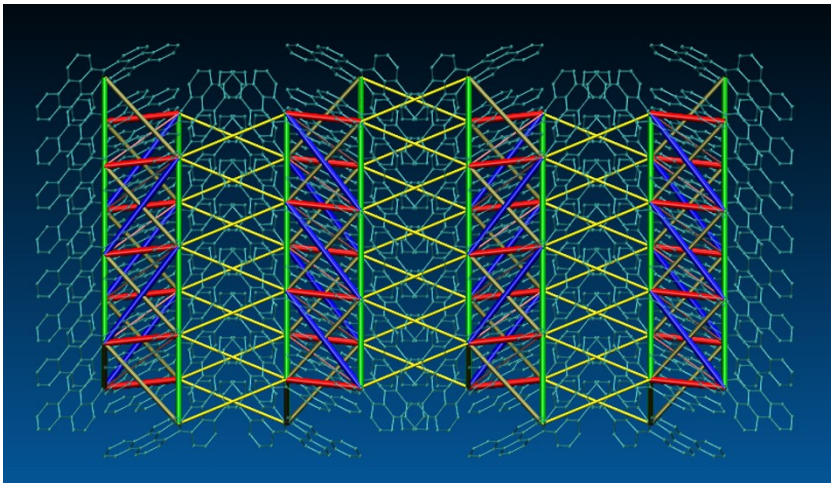

Figure S8. Charge hopping paths in **TBH** lattice.

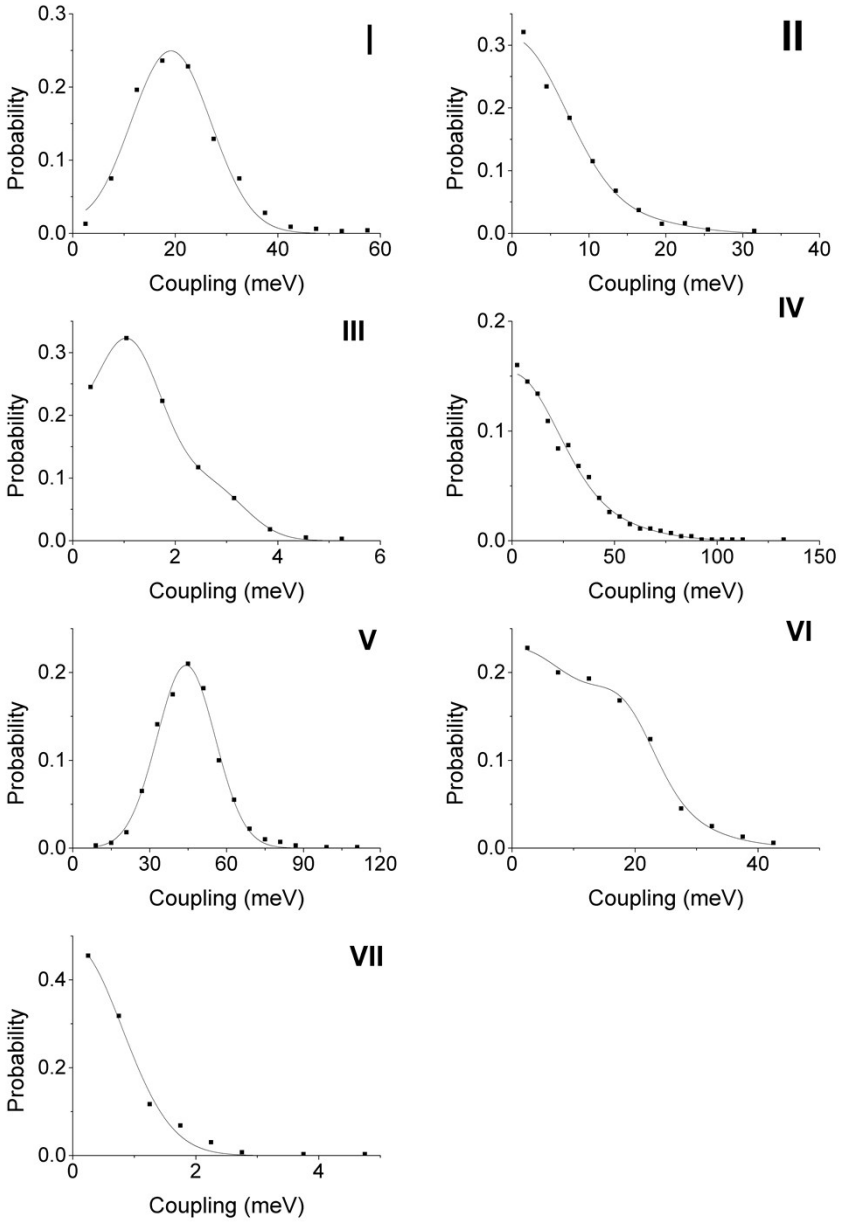

Figure S9. Distributions of the electronic coupling for the charge hopping path in **TBH**.

· **Computational results of TBO**

· **Table S10**. Optimized structures of **TBO**

	Optimized neutral structure			Optimized cationic structure		
	X	Y	Z	X	Y	Z
C	-0.00360	-0.69598	-0.00469	-0.00038	-0.71050	-0.00136
C	-1.25891	-1.38476	-0.29536	-1.23721	-1.38930	-0.31692
C	-1.27403	-2.69220	-0.81957	-1.23652	-2.70051	-0.84413
H	-0.33947	-3.20003	-1.02049	-0.29615	-3.18938	-1.06622
C	-2.46926	-3.31930	-1.13874	-2.43098	-3.33874	-1.15053
H	-2.45787	-4.32333	-1.55404	-2.41943	-4.34063	-1.56786
C	-3.68247	-2.67161	-0.92922	-3.64170	-2.69154	-0.93704
H	-4.59818	-3.20617	-1.15135	-4.55525	-3.22680	-1.16329
C	-3.72612	-1.35082	-0.46551	-3.69975	-1.36051	-0.47134
C	-2.49768	-0.68180	-0.19360	-2.47823	-0.68876	-0.20656
C	-2.48992	0.70664	0.19541	-2.47742	0.69126	0.20524
C	-1.24383	1.39830	0.28732	-1.23563	1.39070	0.31427
C	-1.24405	2.70838	0.80515	-1.23340	2.70234	0.84046
H	-0.30396	3.20880	0.99858	-0.29245	3.19051	1.06164
C	-2.43157	3.34849	1.12710	-2.42706	3.34205	1.14682
H	-2.40843	4.35509	1.53567	-2.41431	4.34442	1.56296
C	-3.65185	2.71051	0.92954	-3.63852	2.69574	0.93485
H	-4.56124	3.25501	1.15333	-4.55142	3.23223	1.16077
C	-3.71030	1.38728	0.47445	-3.69811	1.36419	0.47083
C	-4.99200	0.69584	0.26680	-4.97286	0.67946	0.25099
C	-5.00009	-0.65078	-0.23983	-4.97370	-0.67519	-0.24878
C	-6.22485	-1.26780	-0.47694	-6.19576	-1.30064	-0.48526
H	-6.26068	-2.27946	-0.86591	-6.22981	-2.31549	-0.86491
C	-7.45801	-0.63693	-0.22760	-7.42885	-0.66888	-0.24911
C	-7.44983	0.69644	0.29434	-7.42800	0.67398	0.25732
C	-6.20913	1.31990	0.52412	-6.19413	1.30528	0.49058
H	-6.23274	2.33061	0.91651	-6.22692	2.31989	0.87096
C	-8.69227	1.34160	0.55751	-8.67328	1.32070	0.50412
H	-8.68223	2.35377	0.95529	-8.67060	2.33708	0.88916
C	-9.88139	0.69815	0.31351	-9.85605	0.66850	0.25871
H	-10.82421	1.19883	0.51672	-10.80218	1.16692	0.44800
C	-9.88950	-0.62493	-0.20583	-9.85689	-0.66263	-0.24443
H	-10.83841	-1.12031	-0.39312	-10.80365	-1.16074	-0.43138

C	-8.70830	-1.27511	-0.46976	-8.67495	-1.31521	-0.49277
H	-8.71061	-2.28734	-0.86760	-8.67357	-2.33160	-0.87780
C	0.00360	0.69598	-0.00469	0.00038	0.71050	-0.00136
C	1.25891	1.38476	-0.29536	1.23721	1.38930	-0.31692
C	1.27403	2.69220	-0.81957	1.23652	2.70051	-0.84413
H	0.33947	3.20003	-1.02049	0.29615	3.18938	-1.06622
C	2.46926	3.31930	-1.13874	2.43098	3.33874	-1.15053
H	2.45787	4.32333	-1.55404	2.41943	4.34063	-1.56786
C	3.68247	2.67161	-0.92922	3.64170	2.69154	-0.93704
H	4.59818	3.20617	-1.15135	4.55525	3.22680	-1.16329
C	3.72612	1.35082	-0.46551	3.69975	1.36051	-0.47134
C	2.49768	0.68180	-0.19360	2.47823	0.68876	-0.20656
C	2.48992	-0.70664	0.19541	2.47742	-0.69126	0.20524
C	1.24383	-1.39830	0.28732	1.23563	-1.39070	0.31427
C	1.24405	-2.70838	0.80515	1.23340	-2.70234	0.84046
H	0.30396	-3.20880	0.99858	0.29245	-3.19051	1.06164
C	2.43157	-3.34849	1.12710	2.42706	-3.34205	1.14682
H	2.40843	-4.35509	1.53567	2.41431	-4.34442	1.56296
C	3.65185	-2.71051	0.92954	3.63852	-2.69574	0.93485
H	4.56124	-3.25501	1.15333	4.55142	-3.23223	1.16077
C	3.71030	-1.38728	0.47445	3.69811	-1.36419	0.47083
C	4.99200	-0.69584	0.26680	4.97286	-0.67946	0.25099
C	5.00009	0.65078	-0.23983	4.97370	0.67519	-0.24878
C	6.22485	1.26780	-0.47694	6.19576	1.30064	-0.48526
H	6.26068	2.27946	-0.86591	6.22981	2.31549	-0.86491
C	7.45801	0.63693	-0.22760	7.42885	0.66888	-0.24911
C	7.44983	-0.69644	0.29434	7.42800	-0.67398	0.25732
C	6.20913	-1.31990	0.52412	6.19413	-1.30528	0.49058
H	6.23274	-2.33061	0.91651	6.22692	-2.31989	0.87096
C	8.69227	-1.34160	0.55751	8.67328	-1.32070	0.50412
H	8.68223	-2.35377	0.95529	8.67060	-2.33708	0.88916
C	9.88139	-0.69815	0.31351	9.85605	-0.66850	0.25871
H	10.82421	-1.19883	0.51672	10.80218	-1.16692	0.44800
C	9.88950	0.62493	-0.20583	9.85689	0.66263	-0.24443
H	10.83841	1.12031	-0.39312	10.80365	1.16074	-0.43138
C	8.70830	1.27511	-0.46976	8.67495	1.31521	-0.49277
H	8.71061	2.28734	-0.86760	8.67357	2.33160	-0.87780

Table S11. Distance and electronic coupling of charge hopping path in **TBO**

Type	Distance (Å)	Coupling (meV)
I	3.898	178.5
II	16.089	2.75
III	12.778	0.174
IV	11.987	13.74
V	23.968	-0.148
VI	23.877	0.209

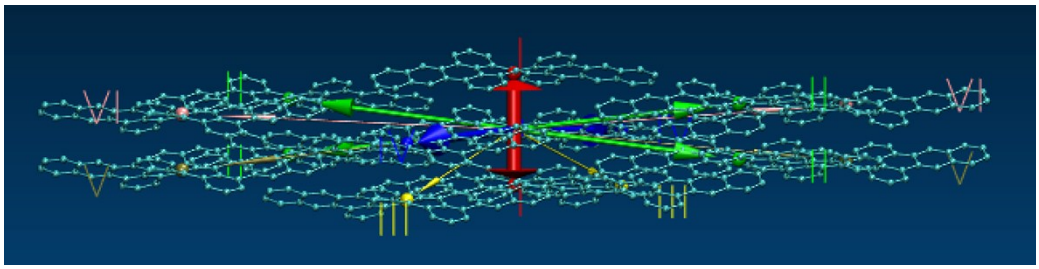

Figure S10. Charge hopping paths of **TBO**.

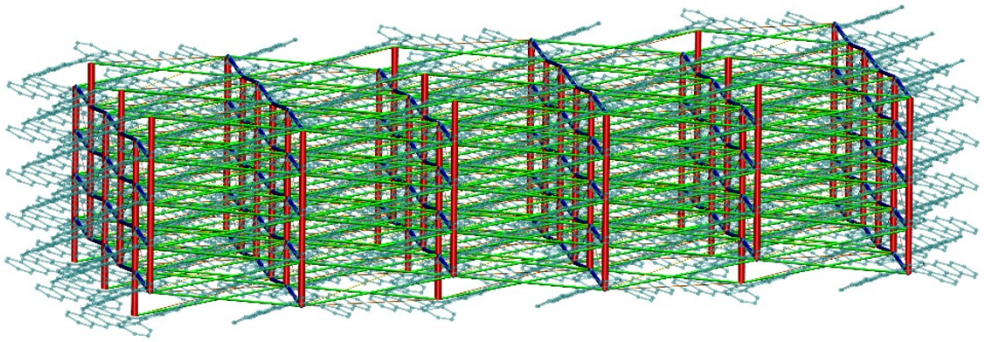

Figure S11. Charge hopping paths in **TBO** lattice.

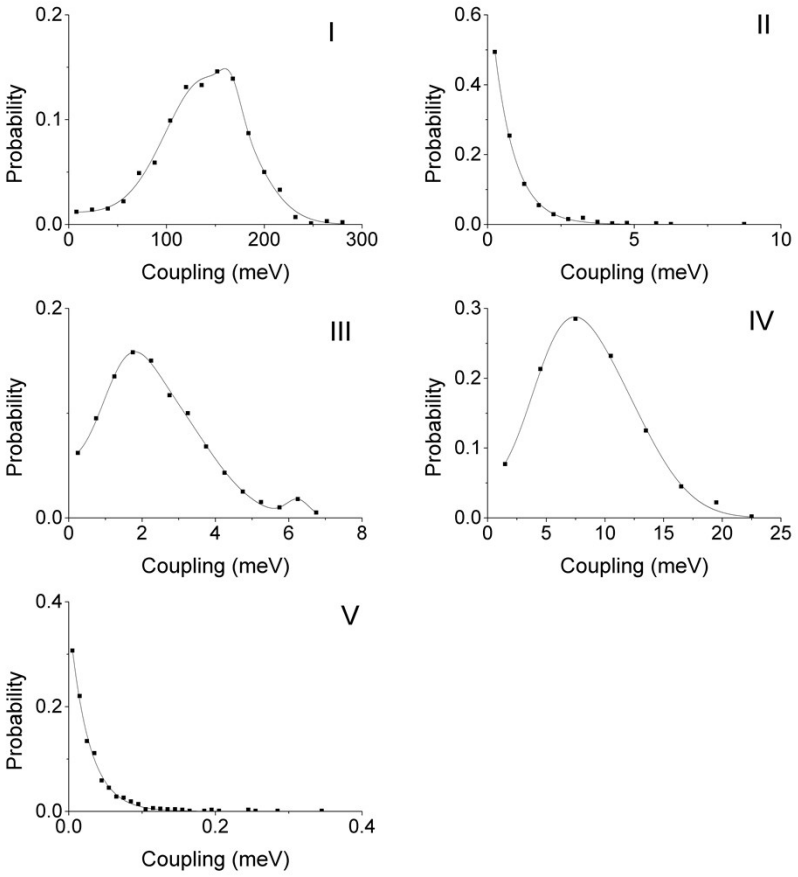

Figure S12. Distributions of the electronic coupling for the charge hopping path in **TBO**.

(D) **Optic microscope images of Crystals**

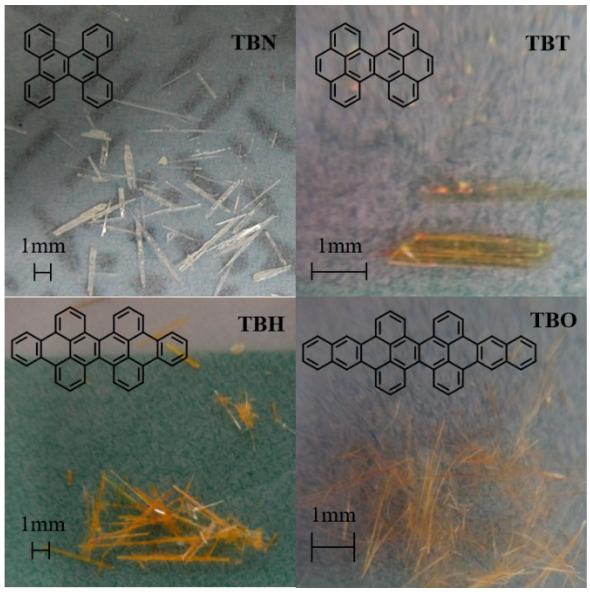

(E) **Device picture, output characteristics and transfer characteristics of SCFET devices**

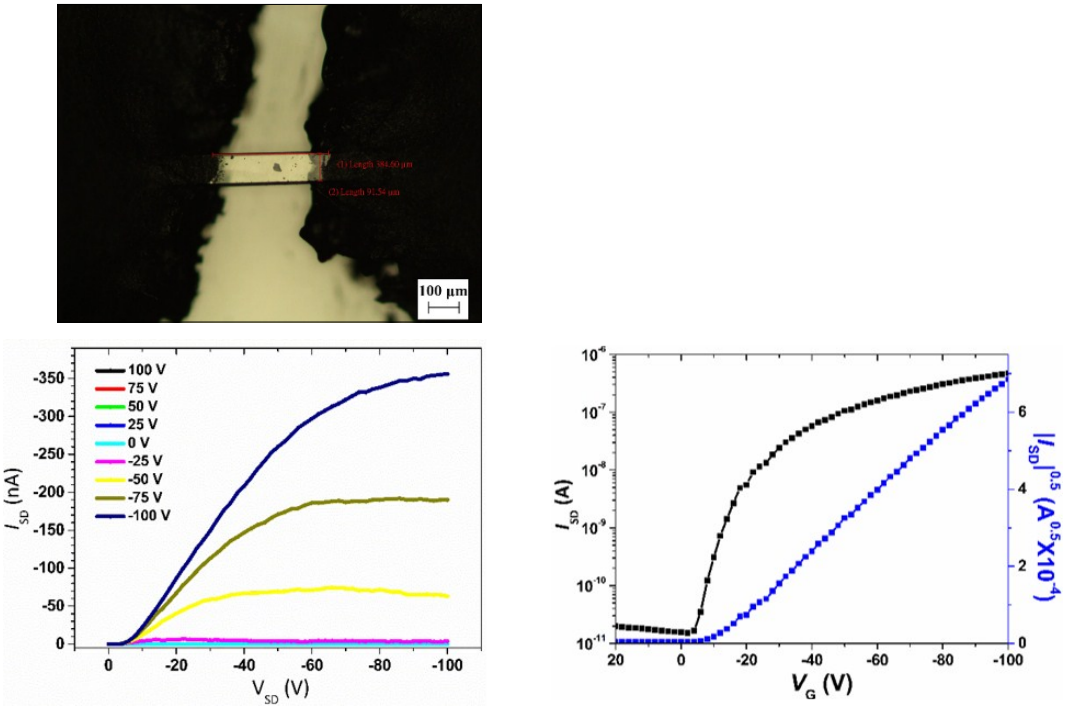

Figure S13. Device picture (scale bar, 100 μm), output characteristics and transfer characteristics of **TBN.** (Values in red in picture are channel length and width)

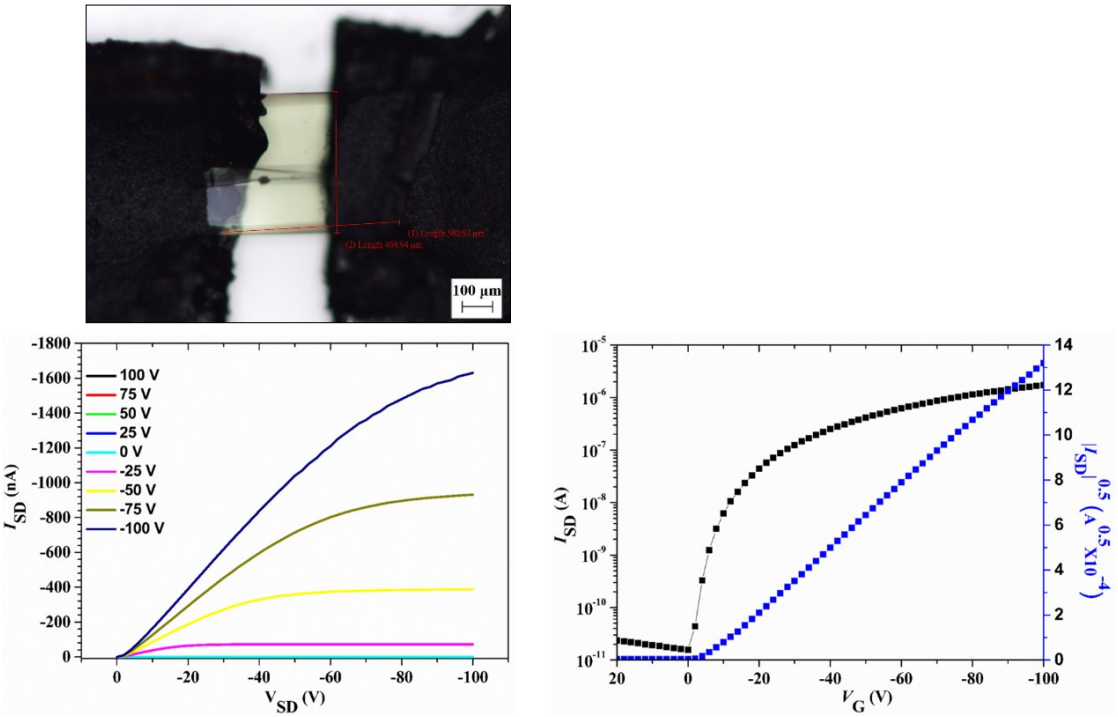

Figure S14. Device picture (scale bar, 100 μm), output characteristics and transfer characteristics of **TBT.** (Values in red in picture are channel length and width)

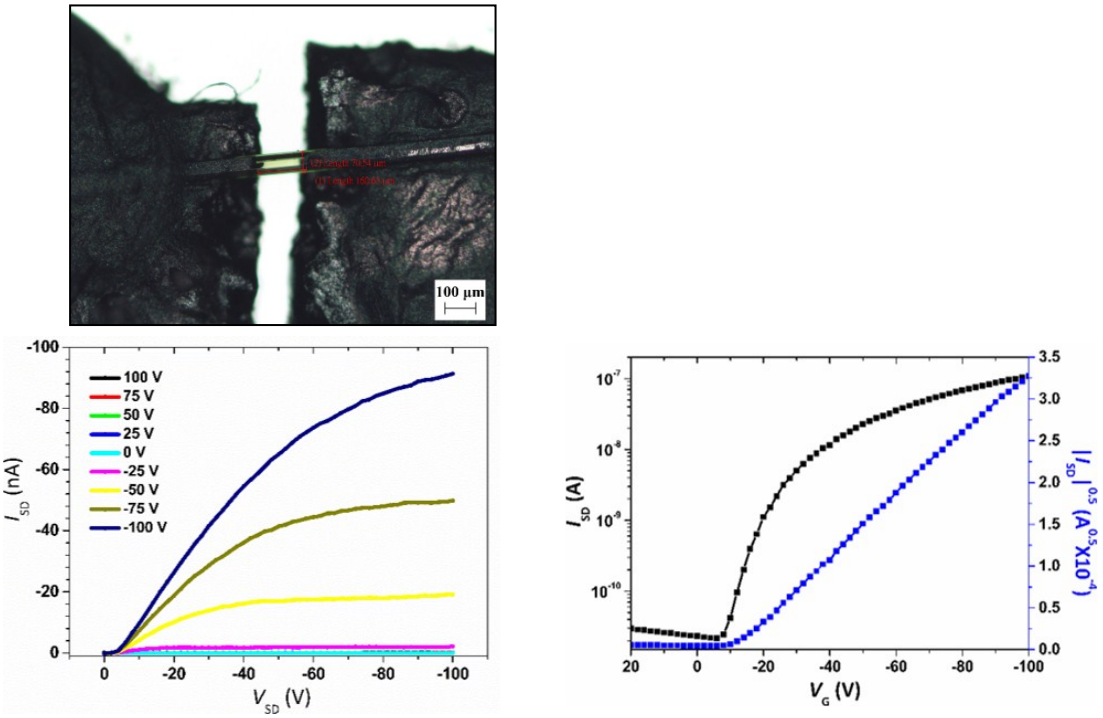

Figure S15. Device picture (scale bar, 100 μm), output characteristics and transfer characteristics of **TBH**. (Values in red in picture are channel length and width).

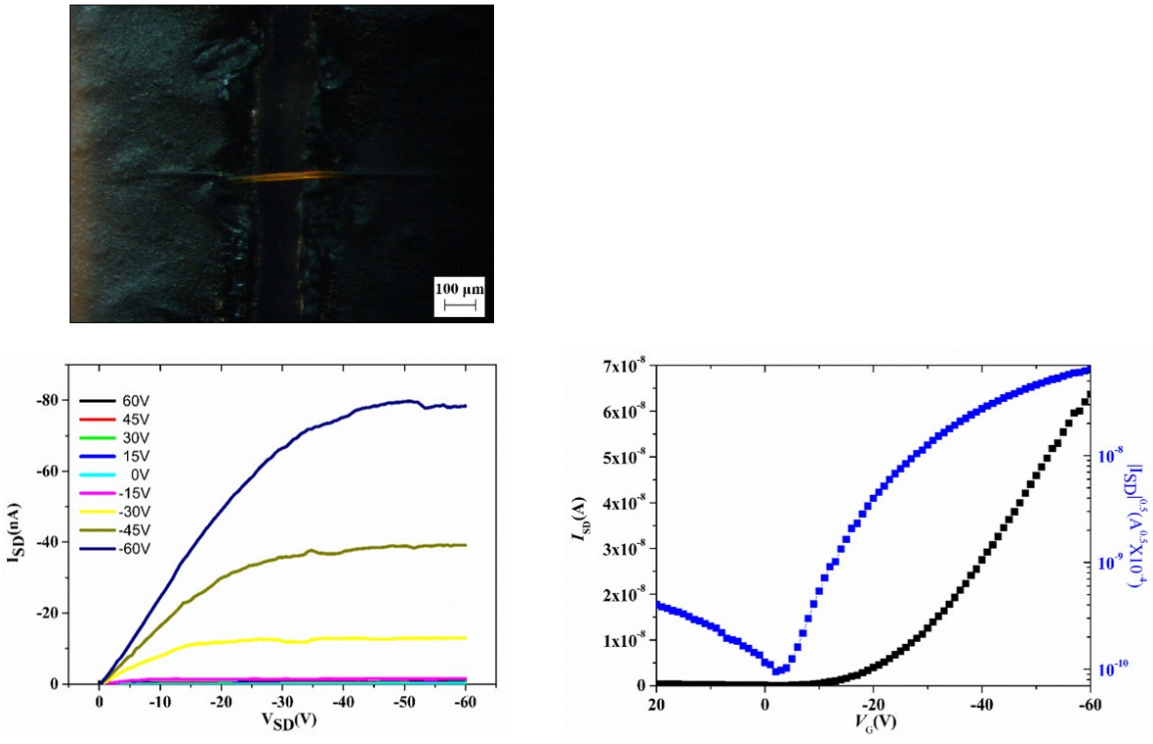

Figure S16. Device picture (scale bar, 100 μm), output characteristics and transfer characteristics of **TBO**

(F) **Reference**

1. Hehre, W. J.; D, R.; Pople, J. A.Self-Consistent Molecular Orbital Methods. XII. Further Extensions of Gaussian-Type Basis Sets for Use in Molecular Orbital Studies of Organic Molecules *J. Chem. Phys.* **1972**, 56, 2257– 2261.
2. Becke, A. D.Density-Functional Thermochemistry. 3. The Role of Exact Exchange. *J. Chem. Phys.* **1993**, 98, 5648– 5652.
3. Lin, B. C.; Cheng, C. P.; Lao, Z. P. M. Reorganization Energies in the Transports of Holes and Electrons in Organic Amines in Organic Electroluminescence Studied by Density Functional Theory. *J. Phys. Chem. A*, **2003**, 107, 5241– 5251.
4. Malagoli, M.; Brédas, J. L. Density Functional Theory Study of the Geometric Structure and Energetics of Triphenylamine-Based Hole-Transporting Molecules. *Chem. Phys. Lett.* **2000**, 327, 13– 17.
5. Farazdel, A.; Dupuis, M.; Clementi, E.; Aviram, A.Electric-Field Induced Intramolecular Electron Transfer in Spiro π-Electron Systems and Their Suitability as Molecular Electronic Devices. a Theoretical Study *J. Am. Chem. Soc.* **1990**, 112, 4206– 4214.
6. Rohrdanz, M. A.; Herbert, J. M.Simultaneous Benchmarking of Ground- and Excited-State Properties with Long-Range-Corrected Density Functional Theory *J. Chem. Phys.* **2008**, 129, 034107– 034109.

7. You, Z.-Q.; Hung, Y.-C.; Hsu, C.-P. Calculating Electron-Transfer Coupling with Density Functional Theory: The Long-Range-Corrected Density Functionals. *J. Phys. Chem. B* **2015**, 119, 7480– 7490.
8. Dunning, T. H., Jr. J. Gaussian Basis Functions for Use in Molecular Calculations. I. Contraction of (9s5p) Atomic Basis Sets for the First-Row Atoms. *Chem. Phys.* **1970**, 52, 2823– 2833.
9. Shao, Y.; Gan, Z.; Epifanovsky, E.; Gilbert, A. T. B.; Wormit, M.; Kussmann, J.; Lange, A. W.; Behn, A.; Deng, J.; Feng, X.; Ghosh, D.; Goldey, M.; Horn, P. R.; Jacobson, L. D.; Kaliman, I.; Khaliullin, R. Z.; Kuś, T.; Landau, A.; Liu, J.; Proynov, E. I.; Rhee, Y. M.; Richard, R. M.; Rohrdanz, M. A.; Steele, R. P.; Sundstrom, E. J.; Woodcock, H. L., III; Zimmerman, P. M.; Zuev, D.; Albrecht, B.; Alguire, E.; Austin, B.; Beran, G. J. O.; Bernard, Y. A.; Berquist, E.; Brandhorst, K.; Bravaya, K. B.; Brown, S. T.; Casanova, D.; Chang, C.-M.; Chen, Y.; Chien, S. H.; Closser, K. D.; Crittenden, D. L.; Diedenhofen, M.; DiStasio, R. A.; Do, H.; Dutoi, A. D.; Edgar, R. G.; Fatehi, S.; Fusti-Molnar, L.; Ghysels, A.; Golubeva-Zadorozhnaya, A.; Gomes, J.; Hanson-Heine, M. W. D.; Harbach, P. H. P.; Hauser, A. W.; Hohenstein, E. G.; Holden, Z. C.; Jagau, T.-C.; Ji, H.; Kaduk, B.; Khistyaev, K.; Kim, J.; Kim, J.; King, R. A.; Klunzinger, P.; Kosenkov, D.; Kowalczyk, T.; Krauter, C. M.; Lao, K. U.; Laurent, A.; Lawler, K. V.; Levchenko, S. V.; Lin, C. Y.; Liu, F.; Livshits, E.; Lochan, R. C.; Luenser, A.; Manohar, P.; Manzer, S. F.; Mao, S.-P.; Mardirossian, N.; Marenich, A. V.; Maurer, S. A.; Mayhall, N. J.; Neuscamman, E.; Oana, C. M.; Olivares-Amaya, R.; O'Neill, D. P.; Parkhill, J. A.; Perrine, T. M.; Peverati, R.; Prociuk, A.; Rehn, D. R.; Rosta, E.; Russ, N. J.; Sharada, S. M.; Sharma, S.; Small, D. W.; Sodt, A.; Stein, T.; Stück, D.; Su, Y.-C.; Thom, A. J. W.; Tsuchimochi, T.; Vanovschi, V.; Vogt, L.; Vydrov, O.; Wang, T.; Watson, M. A.; Wenzel, J.; White, A.; Williams, C. F.; Yang, J.; Yeganeh, S.; Yost, S. R.; You, Z.-Q.; Zhang, I. Y.; Zhang, X.; Zhao, Y.; Brooks, B. R.; Chan, G. K. L.; Chipman, D. M.; Cramer, C. J.; Goddard, W. A., III; Gordon, M. S.; Hehre, W. J.; Klamt, A.; Schaefer, H. F., III; Schmidt, M. W.; Sherrill, C. D.; Truhlar, D. G.; Warshel, A.; Xu, X.; Aspuru-Guzik, A.; Baer, R.; Bell, A. T.; Besley, N. A.; Chai, J.-D.; Dreuw, A.; Dunietz, B. D.; Furlani, T. R.; Gwaltney, S. R.; Hsu, C.-P.; Jung, Y.; Kong, J.; Lambrecht, D. S.; Liang, W. Z.; Ochsenfeld, C.; Rassolov, V. A.; Slipchenko, L. V.; Subotnik, J. E.; van Voorhis, T.; Herbert, J. M.; Krylov, A. I.; Gill, P. M. W.; Head-Gordon, M.Advances in Molecular Quantum Chemistry Contained in the Q-Chem 4 Program Package *Mol. Phys.* **2015**, 113, 184– 215.
10. Allinger, N. L.; Li, F.; Yan, L.; Tai, J. C. Molecular Mechanics (MM3) Calculations on Conjugated Hydrocarbons. *J. Comput. Chem.* **1990**, 11, 868– 895.
11. Lii, J. H.; Allinger, N. L. J.Molecular Mechanics. The MM3 Force Field for

Hydrocarbons. 3. The van der Waals' Potentials and Crystal data for Aliphatic and Aromatic Hydrocarbons *J. Am. Chem. Soc.* **1989**, 111, 8576– 8582.

12. Ponder, J. W.; Richards, F. M.An Efficient Newton-like Method for Molecular Mechanics Energy Minimization of Large Molecules. *J. Comput. Chem.* **1987**, 8, 1016– 1024.
13. Deng, W.; Goddard, W. A.Predictions of Hole Mobilities in Oligoacene Organic Semiconductors from Quantum Mechanical Calculations *J. Phys. Chem. B* **2004**, 108, 8614– 8621.
14. Wen, S.-H.; Li, A.; Song, J.; Deng, W.-Q.; Han, K.-L.; Goddard, W. A., IIIFirst-Principles Investigation of Anistropic Hole Mobilities in Organic Semiconductors *J. Phys. Chem. B* **2009**, 113, 8813– 8819.
15. Bässler, H.Charge Transport in Disordered Organic Photoconductors a Monte Carlo Simulation Study. *Phys. Status Solidi B* **1993**, 175, 15– 56.
16. Fornari, R.; Troisi, A. Theory of Charge Hopping along a Disordered Polymer Chain. *Phys. Chem. Chem. Phys.* **2014**, 16, 9997– 10007.